

Università degli studi di Milano

Thesis
M.Sc. Data Science & Economics

**Bayesian Panel VAR models for
forecasting electricity prices in
Europe**

David A. Fernandez

Code: 988346

Advisor: Luca Rossini

December 18, 2023



UNIVERSITÀ DEGLI STUDI DI MILANO
FACOLTÀ DI SCIENZE POLITICHE,
ECONOMICHE E SOCIALI

A mi madre, Sandra.

Contents

1	Introduction	4
2	Data Structure	7
3	Model Description	17
4	Empirical Results	37
5	Conclusions	50

Abstract

This thesis analyzes the electricity markets in Europe through a Bayesian panel approach. The panel is composed of nine countries from Central, Northern and Southern Europe, with data that ranges from January 2020 to September 2023. A benchmark model with daily electricity price and dummies is tested against other two models that include day-ahead RES generation forecasts data and international fuels and CO₂ prices. Forecasting performance was analyzed using both point and density measures through the Diebold and Mariano test and the Model Confidence Set procedure. Results show that the inclusion of RES and international fuel prices do not provide enough statistical evidence against the benchmark model, and in some cases it even worsens the forecasting capacity of it.

1 Introduction

The last decades have seen a remarkable change in the electricity market in Europe, either because of the liberalization of the market or the increasing penetration of renewable energy sources (RES), or even of geopolitical tensions. As noted by Knittel and Roberts, 2005, restructuring electricity markets removes price control and openly encourages market entry, increasing the importance of modeling and forecasting its prices. To that extent, several studies have been published, continuously improving the set of available tools to assess the behavior of this market. Examples in the literature are the modeling of daily electricity prices in liberalized markets through a multivariate modeling framework (Raviv et al., 2015); modeling of low frequency macroeconomic variables and high frequency electricity prices altogether (Foroni et al., 2023); and smoothing quantile regression averaging for probabilistic forecasting (Uniejewski, 2023).

Moreover, particular interest has been developed in understanding the impact of

RES penetration in electricity markets. Among the recent developments, Durante et al., 2022, examine the dependence between electricity prices, demand, and RES in Germany; or Gianfreda et al., 2023, model hourly-prices by including regressors such as fuel prices, forecasted demand and forecasted RES, using Bayesian time-varying volatility models for Germany, Italy, and Denmark.

Despite the latest innovations found in research, not much is available related to panel modeling of electricity prices in Europe. Studying the market through a panel approach could indicate up to which extent the markets are interconnected and measure their interdependencies. In this sense, this thesis seeks to integrate some of the latest studies and propose an application of Bayesian panel modeling with the aim of understanding the cross-country effects of the market, the effect of RES penetration on its pricing, and finally producing three different forecasts on the day-ahead electricity prices. Expected results are larger coefficients for larger markets, as they have a bigger infrastructure and therefore could influence greatly the overall European market; and a considerable improvement in the forecasting accuracy when exogenous variables are included, especially for units with high RES penetration on their generation matrix.

For this purpose, daily electricity prices (EUR/MWh) are modeled through a time series Bayesian Panel VAR (BVAR) composed of nine countries (units): Belgium, Denmark, France, Finland, Germany, Italy, the Netherlands, Portugal, and Spain, following the structural factor model proposed by Dieppe et al., 2016 under section 6.7, which follows the Bayesian Panel factor approach developed by Ciccarelli and Canova, 2006 and Canova and Ciccarelli, 2013.

Three different models are tested: first, a panel BVAR with daily electricity prices as the only explanatory variable, plus dummies; second, a panel BVAR which includes the RES day-ahead forecast for every unit for solar generation (MW), wind generation (MW), and total system load (MW), and dummies; and third, a panel BVARX which, on top of the last model, includes daily international prices of fuels such as oil, gas, coal, and CO₂ prices.

Each model is fitted first on an in-sample period that ranges from January 1st, 2021 to December 31st, 2021 and coefficients of the different approaches are analysed. Then, an out-of-sample period that ranges from January 1st, 2022 to September 30th, 2023 is used to produce a daily rolling-window Bayesian forecast for every model; forecasts are evaluated by using both point estimate measures (RMSE ¹) and density measures (CRPS ²), employed both in the Diebold and Mariano test (Diebold and Mariano, 1995) with Newey-West standard errors and the Model Confidence Set (Hansen et al., 2011) procedure.

The dataset was built during March 2023 and updated in October 2023, and it is composed of the hourly electricity prices for each country (unit), which were sourced from the Refinitiv³ market tool, with the exception of Italy, for which the electricity prices were sourced from the GME (Gestore Mercati Energetici)⁴ web platform. Data on oil, gas, coal, and CO2 prices was also gathered from Refinitiv, as well as exchange rates to convert prices to EUR. On the other hand, data on day-ahead RES generation forecast and day-ahead total load forecast were gathered from ENTSO-E Transparency platform ⁵.

The rest of the thesis is structured as follows. Section 2 describes the data pre-processing phase and analyses the data before modeling, Section 3 describes the modeling approach of the three different Bayesian Panel VARs. Section 4 comments on the in-sample analysis as well as the forecasts produced for the models tested. Finally, conclusions are discussed in Section 5.

¹Root Mean Square Error

²Continuous Ranking Probability Score

³Access granted through the University of Milan's library services

⁴Available at [GME](#).

⁵Available at [ENTSO-E Transparency](#)

2 Data Structure

The study relies on a database composed of the following variables for each of the units in the panel, with daily frequency: *electricity price (EUR/MWh)*, *forecasted day-ahead solar generation (MW)*, *forecasted day-ahead wind generation (MW)*, and *forecasted day-ahead load (MW)*; the following variables which are exogenous to all the units, with daily frequency as well, prices for: *oil (EUR/barrel)*, *gas (EUR/therm)*, *coal (EUR/metric tone)*, and *CO2 (EUR/metric tone)*. The dataset ranges from January 1st, 2020, to September 30th, 2023, for nine different countries, composing a balanced panel.

It is worth noticing that the daily electricity price series for each unit was built from the hourly series, by averaging the 24 datapoints of each day. For some units, data was not present for some days, holidays or weekends, in which case the series was completed using the *forecasted day-ahead electricity price* published by ENTSO-E Transparency.

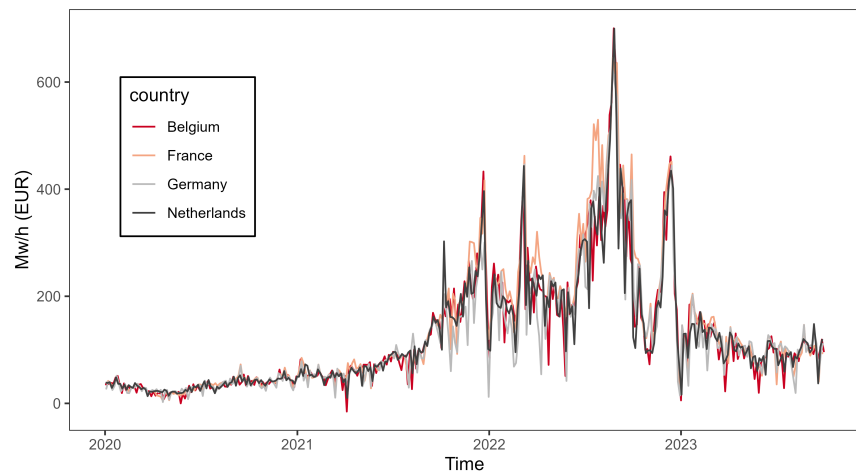
All data on electricity prices was collected from the Refinitiv data tool from Thomson Reuters, which gathers the data from the corresponding exchange market of each country. Note that the Danish market is split into two zones, East and West, therefore the final price for the country is the average between both zones. Table 1 maps each unit and it's corresponding exchange.

Table 1: Market Exchange for the electricity market, per country

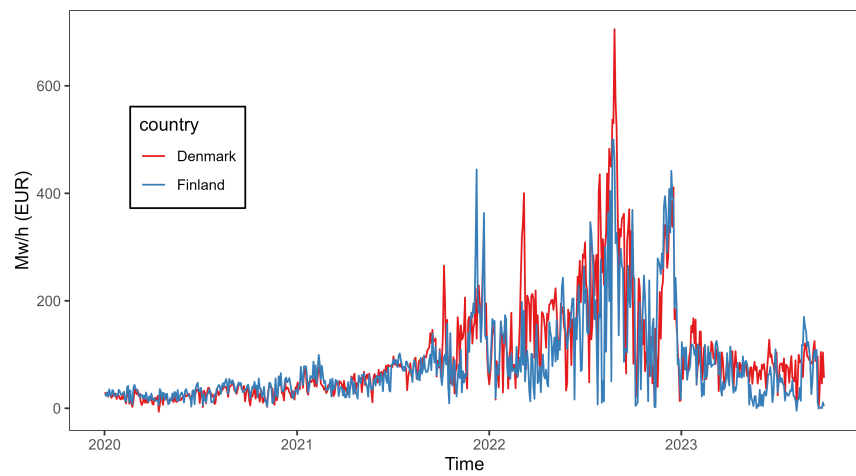
Country	Exchange	Magnitude
Belgium	BPX Fix Hour	EUR/MWh
Denmark	NordPool East Denmark	EUR/MWh
Denmark	Nordpool West Denmark	EUR/MWh
Finland	Nordpool Finland	EUR/MWh
France	Powernext Elec.Hour	EUR/MWh
Germany	EEX - Hourly Spot Hour	EUR/MWh
Italy	GME Italy Hourly	EUR/MWh
Netherlands	EPX - Electricity Spot NL	EUR/MWh
Portugal	OMEL - Elec. Portugal	EUR/MWh
Spain	OMEL - Elec. Spain	EUR/MWh

Figure 1 shows the daily average of the hourly electricity prices in EUR for all the units, split in three different plots according to each unit location: Belgium (BE), France (FR), Germany (DE), and the Netherlands (NL) represent Central Europe; Denmark (DK) and Finland (FI), Northern Europe; Italy (IT), Portugal (PT), and Spain (SP), Southern Europe.

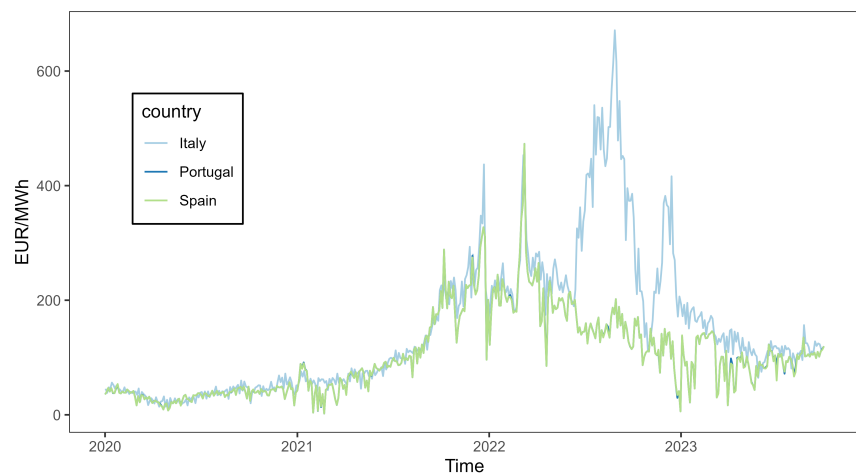
It is clearly evident throughout all countries the low-volatility period that ranges from 2020 up to the second quarter of 2021, when the demand rose quickly after the recovery from Covid related restrictions, then the Russian invasion of Ukraine took place in February 2022, which, among other factors, contributed to the soaring of the prices and their peaks in different points in time. Moreover, it can be seen how the electricity price in Portugal and Spain didn't reach a peak after Russian invasion, allowing for a faster return to previous levels. For the rest of the panel, it is only during the first months of 2023 that prices seem to get back to the levels they were around the first quarter of 2021.



(a) BE, FR, DE, NL



(b) DK, FI



(c) IT, PT, SP

Figure 1: Electricity price (EUR/MWh) per country

When looking at the correlation matrix of the electricity price of each country for the period 2020 to 2021 in Figure 2, it is clearly seen the close relation between electricity markets of Portugal and Spain, which are virtually the same, while, on the other hand, markets as Finland are the less correlated with the rest of the countries in the panel. It can also be noted how highly correlated are the markets in central Europe: Belgium, France, Germany, and the Netherlands, and despite Denmark being a Nordic country, it is less correlated with Finland. Finally, Italy shows high correlation coefficients both with countries in central and southern Europe, and a low correlation with Denmark and Finland.

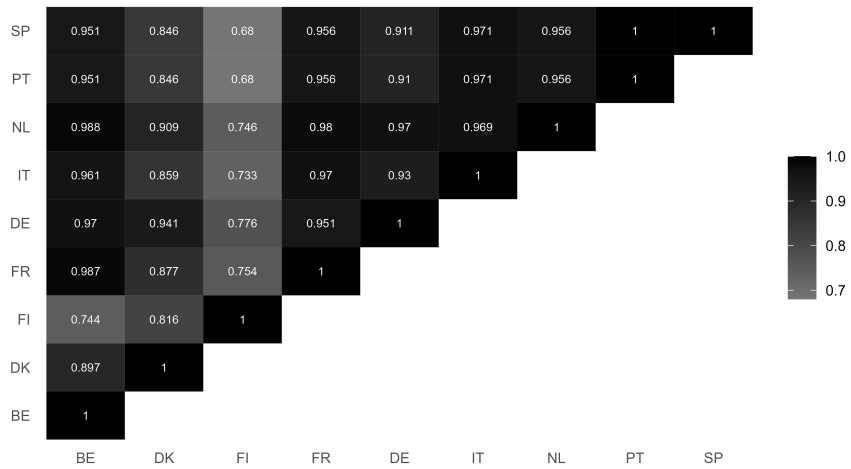


Figure 2: Correlation matrix, electricity price (EUR/MWh), in-sample period [2020 - 2021]

As the in-sample period does not include the events unfolded in Ukraine during February 2023, it is not evident its effect in the correlation structure of the electricity prices. To better analyze these changes, the coefficients of a 28-day rolling-window correlation matrix for the whole sample period were computed for the panel. In this section, Figures 3 and 4 depict the results for Germany and France, respectively, but all charts are available at the Appendix at the end of the document.

When looking at Germany's correlation coefficients evolution, it is seen how the correlation against France was affected during the first months of 2022, and how,

precisely after this period, the correlation with Belgium and the Netherlands became less volatile and closer to 1. Despite not having a stable trend even before Russian invasion of Ukraine, the correlation of Germany's electricity price against Italy, Spain, and Portugal does seem to become more volatile and farther away from 1 after the first quarter of 2022.

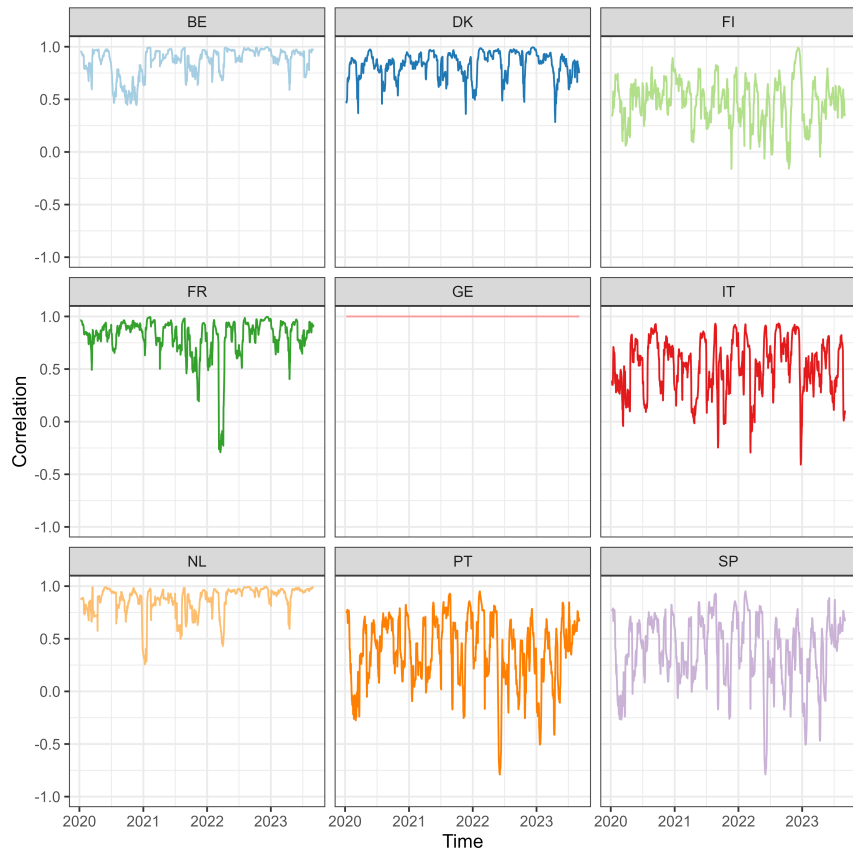


Figure 3: Rolling-window correlation coefficients [2020-2023]: Germany

Different results are seen for France. Correlation dropped considerable against all the countries in the panel, except of Italy, around the first quarter of 2022. The drops in correlation are relative to each country. Highest reductions are seen against Portugal and Spain, with a posterior stabilisation of the correlation at lower levels than in 2020 and 2021. Against Belgium, Germany and the Netherlands, correlation went back to pre-war levels relatively quickly. Against Finland it is clearly seen how the volatility of the correlation increases from 2022, as well as with Den-

mark, although not that clearly visible.

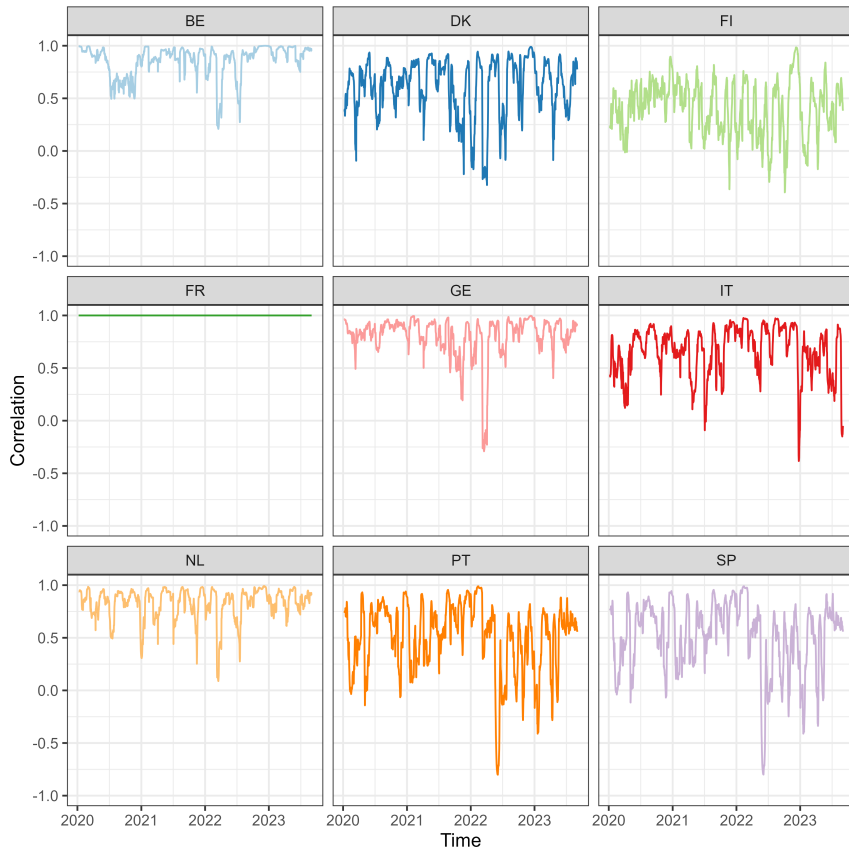


Figure 4: Rolling-window correlation coefficients [2020-2023]: France

Data on day-ahead generation forecasts was collected from the European network of the transmission system operators for electricity (ENTSOE). The day-ahead forecasts on electricity generation from wind and solar photo-voltaic plants are published at 6:00 p.m. (Brussels time) every day, although additional information is also provided through their *current* and *intraday* forecasts, which represent the last current update done at 8:00 a.m., for all 24h of the day.

Day-ahead generation forecasts for solar, wind, and load were averaged accordingly, as for every unit the reported frequency would vary from 15-minutes up to hourly frequency. In the case NA's were found, depending on the availability of adjacent datapoints, a simple average, a 2x2 system of equations or a spline interpolation was implemented; it must be noted that the spline interpolation was

needed only for three values of the solar generation series for Portugal in June 2023.

Figure 5 shows the corresponding graphs for day-ahead generation series. Seasonal patterns are recognizable as well as the capabilities in generation each unit has depending on the type of energy.

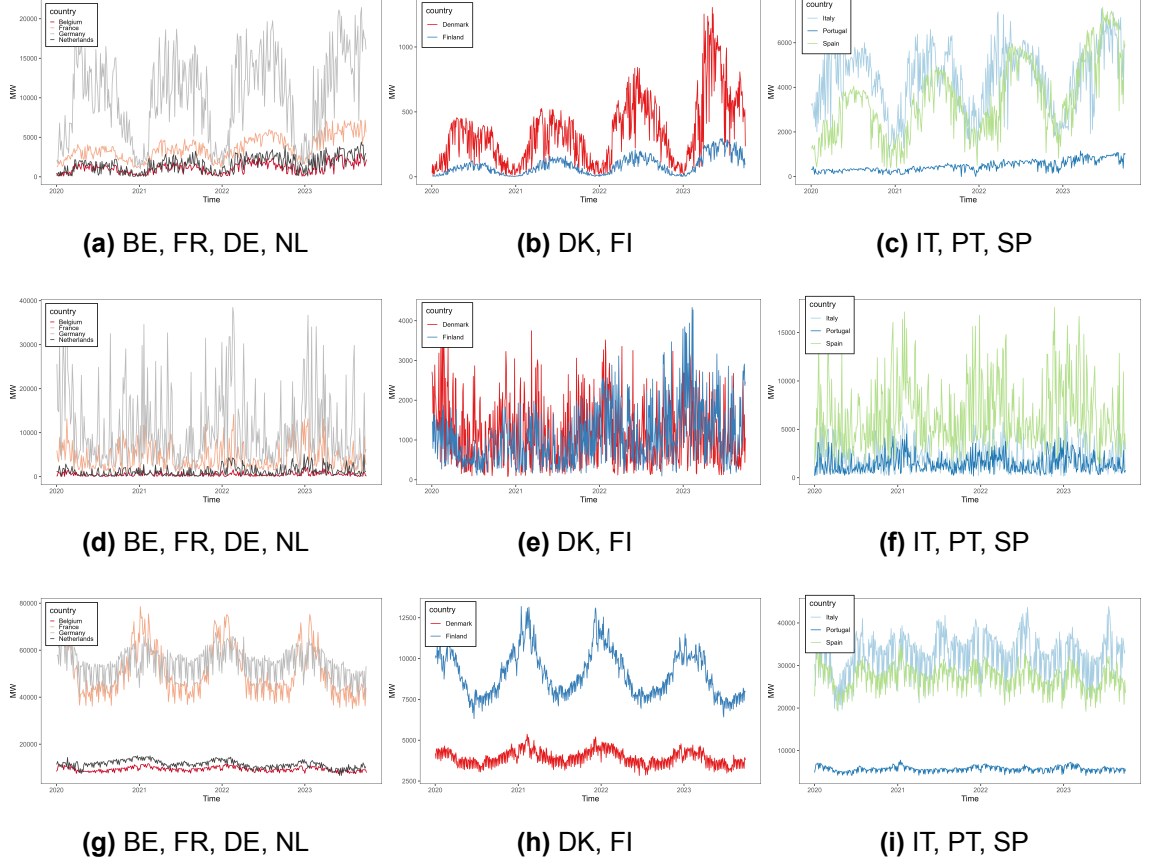


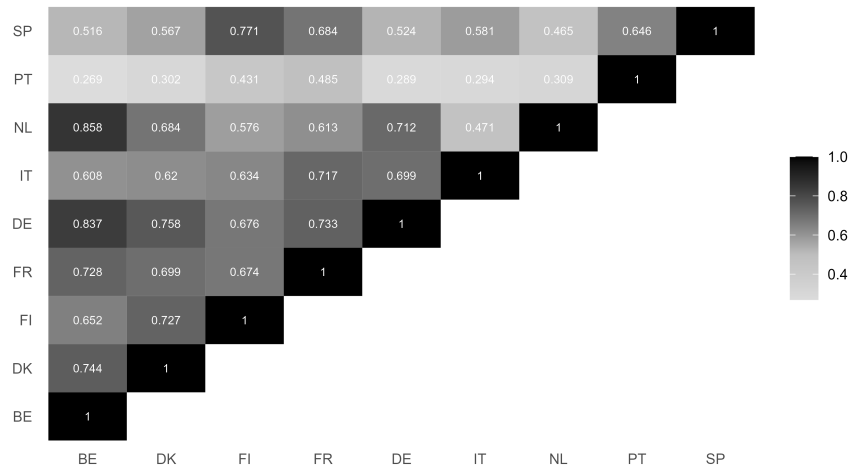
Figure 5: Day-ahead forecasts (MW) for solar (top row), wind (middle row), and load (bottom row).

Correlation matrices for day-ahead generation forecasts for solar, wind and load are displayed in Figure 6 for the period 2020 - 2021. With respect with solar generation, higher correlations are between Belgium and the Netherlands, and Belgium and Germany. Here, Denmark is better correlated with Finland and Portugal is the less correlated with the rest of the panel. This behaviors may be explained by the total

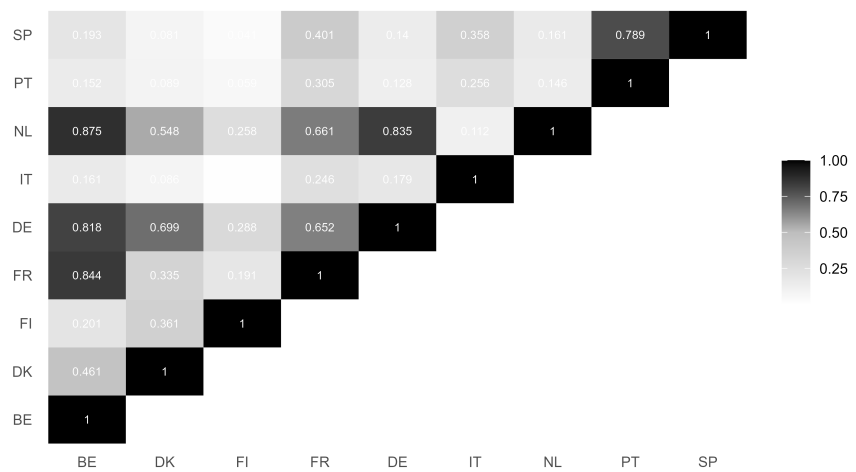
capacity in solar generation that each country it may have, this is, the larger the installed capacity, the greater room for variation is, so small countries are relatively stable as their capacity is filled in relatively quickly compared with bigger countries.

Correlation matrix on day-ahead wind generation forecast shows even a greater geographical influence on the data, with Spain being highly correlated with Portugal but no other country, the Netherlands correlated with Germany and Belgium, Italy with practically no considerable correlation with any country in the panel and France only correlated considerably with Belgium.

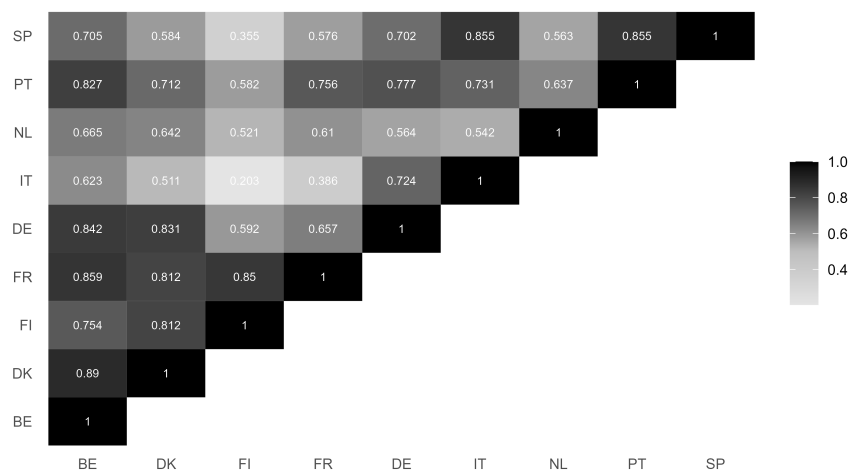
Finally, the day-ahead load forecast correlation matrix is somewhat similar to the already discussed electricity price correlation matrix. Geographical proximity explains part of the data, as for example Finland and Italy show the lower correlations, as they are the ones that share the lesser length in borders with the other countries in the panel (even no borders). Nonetheless, Spain and Italy are highly correlated, as well as Portugal and Belgium, and Belgium and the Netherlands show a relatively low coefficient, despite being neighbouring countries of similar size.



(a) Solar



(b) Wind



(c) Load

Figure 6: Day-ahead generation forecasts (MW) correlation matrices, in-sample period [2020-2021]

Regarding international fuels and CO₂ prices, they were gathered as well from Refinitiv, using the quotes showed in Table 2, the series were converted into EUR when needed. Figure 7 displays the time series plots in EUR of the fuels and CO₂. Oil, Gas and Coal prices depict the same hike when the Russian invasion of Ukraine happened, with Oil price not going back to pre-war levels. CO₂ price shows also a stable trend since beginning of 2022 and no signal of decreasing toward 2020 or 2021 levels.

Table 2: Quotations for fuels and CO₂ prices

Fuel	Quote	Price
Oil	Crude Oil-WTI Spot Cushing	USD/barrel
Gas	ICE Natural Gas 1 Mth.Fwd	BPN/therm
Coal	Coal ICE API2 CIF ARA Nr	USD/metric tone
CO ₂	EEX-EU CO ₂ Emissions E/EUA	EUR/metric tone

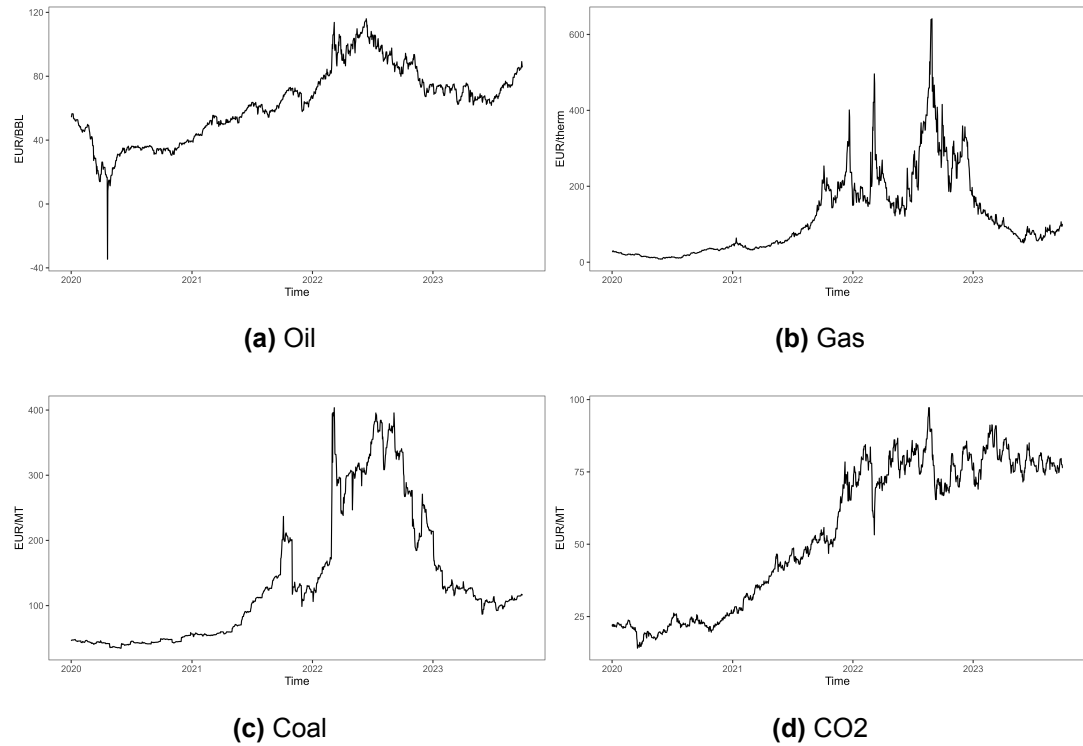


Figure 7: International fuels and CO₂ daily price (EUR)

3 Model Description

Panel VAR model

It is in our interest to understand how the different electricity markets are interconnected and what role they play in the different units the panel is composed of, as well as determining which set of variables improves the forecasting accuracy of electricity prices the most. This study explores the use of a Panel Bayesian vector autoregressive (BVAR) model to answer these questions, describing three models: 1) a panel BVAR with electricity price as endogenous variable, including dummies, 2) a panel BVARX model which adds forecasted RES generation (solar, wind, load) at time t per unit on top of model 1), and, 3) a panel BVARX which builds on top of model 2) and includes international daily prices (at $t - 1$) for fuels and CO₂, which are exogenous to all units in the panel.

We initially describe the structure of a panel VAR, where i denotes the unit (country) ($i = 1, \dots, N$), t the time periods ($t = 1, \dots, T$), and j the lags of the VAR model ($j = 1, \dots, p$). From Dieppe et al., 2016, a panel VAR for unit i ($i = 1, 2, \dots, N$) can be described in its most general form as:

$$\begin{aligned} y_{it} &= \sum_{i=1}^N \sum_{j=1}^p A_{ij,t}^k y_{j,t-k} + C_{i,t} x_t + \varepsilon_{it} \\ &= A_{i1,t}^1 y_{1,t-1} + \dots + A_{i1,t}^p y_{1,t-p} \\ &\quad + A_{i2,t}^1 y_{2,t-1} + \dots + A_{i2,t}^p y_{2,t-p} \\ &\quad + \dots \\ &\quad + A_{iN,t}^1 y_{N,t-1} + \dots + A_{iN,t}^p y_{N,t-p} \\ &\quad + C_{i,t} x_t + \varepsilon_{it} \end{aligned} \tag{1}$$

with:

$$y_{i,t} = \underbrace{\begin{pmatrix} y_{i1,t} \\ y_{i2,t} \\ \vdots \\ y_{in,t} \end{pmatrix}}_{n \times 1}, A_{ij,t}^k = \underbrace{\begin{pmatrix} a_{ij,11,t}^k & a_{ij,12,t}^k & \cdots & a_{ij,1n,t}^k \\ a_{ij,21,t}^k & a_{ij,22,t}^k & \cdots & a_{ij,2n,t}^k \\ \vdots & \vdots & \ddots & \vdots \\ a_{ij,n1,t}^k & a_{ij,n2,t}^k & \cdots & a_{ij,nn,t}^k \end{pmatrix}}_{n \times n},$$

$$C_{it} = \underbrace{\begin{pmatrix} c_{i1,1t} & c_{i1,2t} & \cdots & c_{i1,mt} \\ c_{i2,1t} & c_{i2,2t} & \cdots & c_{i2,mt} \\ \vdots & \vdots & \ddots & \vdots \\ c_{in,1t} & c_{in,2t} & \cdots & c_{in,mt} \end{pmatrix}}_{n \times m}, x_t = \underbrace{\begin{pmatrix} x_{1,t} \\ x_{2,t} \\ \vdots \\ x_{m,t} \end{pmatrix}}_{m \times 1}, \epsilon_{i,t} = \underbrace{\begin{pmatrix} \varepsilon_{i1,t} \\ \varepsilon_{i2,t} \\ \vdots \\ \varepsilon_{in,t} \end{pmatrix}}_{n \times 1}$$

where $y_{i,t}$ denotes a $n \times 1$ vector comprising the n endogenous variables of unit i at time t , while $y_{ij,t}$ is the j^{th} endogenous variable of unit i . $A_{ij,t}^k$ is a $n \times n$ matrix of coefficients providing the response of unit i to the k^{th} lag of unit j at period t . For matrix $A_{ij,t}^k$, the coefficient $a_{ij,lm,t}^k$ gives the response of variable l of unit i to the k^{th} lag of variable m of unit j . x_t is the $m \times 1$ vector of exogenous variables, and C_{it} is the $n \times m$ matrix relating the endogenous variables to these exogenous variables. For C_{it} , the coefficient $c_{ij,l,t}$ gives the response of endogenous variable j of unit i to the l^{th} exogenous variable. Finally, $\varepsilon_{i,t}$ denotes a $n \times 1$ vector of residuals for the variables of unit i , with the following properties:

$$\varepsilon_{it} \sim \mathcal{N}(0, \Sigma_{ii,t})$$

with:

$$\begin{aligned}
\Sigma_{ii,t} &= \mathbb{E}(\varepsilon_{i,t}\varepsilon'_{i,t}) = \mathbb{E} \left(\begin{pmatrix} \varepsilon_{i,1,t} \\ \varepsilon_{i,2,t} \\ \vdots \\ \varepsilon_{i,n,t} \end{pmatrix} \left(\begin{matrix} \varepsilon'_{i,1,t} & \varepsilon'_{i,2,t} & \dots & \varepsilon'_{i,n,t} \end{matrix} \right) \right) \\
&= \underbrace{\begin{pmatrix} \sigma_{ii,11,t} & \sigma_{ii,12,t} & \dots & \sigma_{ii,1n,t} \\ \sigma_{ii,21,t} & \sigma_{ii,22,t} & \dots & \sigma_{ii,2n,t} \\ \vdots & \vdots & \ddots & \vdots \\ \sigma_{ii,n1,t} & \sigma_{ii,n2,t} & \dots & \sigma_{ii,nn,t} \end{pmatrix}}_{n \times n}, \tag{2}
\end{aligned}$$

where $\varepsilon_{i,t}$ is assumed to be non-autocorrelated, so that $\mathbb{E}(\varepsilon_{i,t}\varepsilon'_{i,t}) = \Sigma_{ii,t}$, while $\mathbb{E}(\varepsilon_{i,t}\varepsilon'_{i,s}) = 0$ when $t \neq s$. Note that in this general setting the variance-covariance matrix for the VAR residuals is allowed to be period-specific, which implies a general form of heteroskedasticity.

For each variable in unit i , the dynamic equation at period t contains a total of $k = Nnp + m$ coefficients to estimate, implying $q = n(Nnp + m)$ coefficients to estimate for the whole unit. Stacking over the N units, the model can be reformulated in stacked form as:

$$\begin{aligned}
y_{it} &= \sum_{j=1}^p A_t^k y_{t-k} + C_t x_t + \varepsilon_t \\
&= A_t^1 y_{t-1} + \dots + A_t^p y_{t-p} + C_t x_t + \varepsilon_t
\end{aligned} \tag{3}$$

while in an extended form as:

$$\begin{aligned}
y_{i,t} &= \begin{pmatrix} y_{1,t} \\ y_{2,t} \\ \vdots \\ y_{N,t} \end{pmatrix} = \begin{pmatrix} A_{11,t}^1 & A_{12,t}^1 & \dots & A_{1N,t}^1 \\ A_{21,t}^1 & A_{22,t}^1 & \dots & A_{2N,t}^1 \\ \vdots & \vdots & \ddots & \vdots \\ A_{N1,t}^1 & A_{N2,t}^1 & \dots & A_{NN,t}^1 \end{pmatrix} \begin{pmatrix} y_{1,t-1} \\ y_{2,t-1} \\ \vdots \\ y_{N,t-1} \end{pmatrix} + \dots \\
&\quad + \begin{pmatrix} A_{11,t}^p & A_{12,t}^p & \dots & A_{1N,t}^p \\ A_{21,t}^p & A_{22,t}^p & \dots & A_{2N,t}^p \\ \vdots & \vdots & \ddots & \vdots \\ A_{N1,t}^p & A_{N2,t}^p & \dots & A_{NN,t}^p \end{pmatrix} \begin{pmatrix} y_{1,t-p} \\ y_{2,t-p} \\ \vdots \\ y_{N,t-p} \end{pmatrix} + \begin{pmatrix} C_{1,t} \\ C_{2,t} \\ \vdots \\ C_{N,t} \end{pmatrix} x_t + \begin{pmatrix} \varepsilon_{1,t} \\ \varepsilon_{2,t} \\ \vdots \\ \varepsilon_{N,t} \end{pmatrix}
\end{aligned} \tag{4}$$

with:

$$\begin{aligned}
y_{i,t} &= \underbrace{\begin{pmatrix} y_{1,t-p} \\ y_{2,t-p} \\ \vdots \\ y_{N,t-p} \end{pmatrix}}_{N \times 1}, A_t^k = \underbrace{\begin{pmatrix} A_{11,t}^k & A_{12,t}^k & \dots & A_{1N,t}^k \\ A_{21,t}^k & A_{22,t}^k & \dots & A_{2N,t}^k \\ \vdots & \vdots & \ddots & \vdots \\ A_{N1,t}^k & A_{N2,t}^k & \dots & A_{NN,t}^k \end{pmatrix}}_{N \times Nn}, \\
C_t &= \underbrace{\begin{pmatrix} C_{1,t} \\ C_{2,t} \\ \vdots \\ C_{N,t} \end{pmatrix}}_{N \times m}, \epsilon_t = \underbrace{\begin{pmatrix} \varepsilon_{1,t} \\ \varepsilon_{2,t} \\ \vdots \\ \varepsilon_{N,t} \end{pmatrix}}_{N \times 1}.
\end{aligned} \tag{5}$$

As stated previously, the vector of residuals ε_t has the following properties:

$$\varepsilon_t \sim \mathcal{N}(0, \Sigma_t), \tag{6}$$

with:

$$\begin{aligned}
\Sigma_t &= \mathbb{E}(\varepsilon_t \varepsilon'_t) = \mathbb{E} \left(\begin{pmatrix} \varepsilon_{1,t} \\ \varepsilon_{2,t} \\ \vdots \\ \varepsilon_{N,t} \end{pmatrix} \begin{pmatrix} \varepsilon'_{1,t} & \varepsilon'_{2,t} & \dots & \varepsilon'_{N,t} \end{pmatrix} \right) \\
&= \underbrace{\begin{pmatrix} \Sigma_{11,t} & \Sigma_{12,t} & \dots & \Sigma_{1N,t} \\ \Sigma_{21,t} & \Sigma_{22,t} & \dots & \Sigma_{2N,t} \\ \vdots & \vdots & \ddots & \vdots \\ \Sigma_{N1,t} & \Sigma_{N2,t} & \dots & \Sigma_{NN,t} \end{pmatrix}}_{Nn \times Nn} \quad (7)
\end{aligned}$$

The assumption of absence of autocorrelation is then extended to the whole model: $\mathbb{E}(\varepsilon_t \varepsilon'_s) = \Sigma_t$ while $\mathbb{E}(\varepsilon_t \varepsilon'_s) = 0$ when $t \neq s$. Equation (3) implies that there are $h = Nq = Nn(Nnp + m)$ coefficients to estimate.

The formulation in equation (3) is the most general form of a panel VAR model, and, it is characterised by four properties on interdependency and heterogeneity:

1. Dynamic interdependencies: the dynamic behaviour of each unit is determined by lagged values of itself, but also by lagged values of all the other endogenous variables of all other units. In other words, the matrix of coefficients $A_{ij,t}^k \neq 0$ when $i \neq j$, for $k = 1, \dots, p$ and $t = 1, \dots, T$.
2. Static interdependencies: the error terms $\varepsilon_{i,t}$ are allowed to be correlated across units. That is, in general, $\Sigma_{ij,t} \neq 0$ when $i \neq j$, and $t = 1, \dots, T$.
3. Cross-subsectional heterogeneity: the VAR coefficients and residual variances are allowed to be unit-specific. In other words, $A_{ij,t}^k \neq A_{lj,t}^k$, $C_{i,t} \neq C_{j,t}$ and $\Sigma_{ii,t} \neq \Sigma_{jj,t}$ when $i \neq j$, where $k = 1, \dots, p$, $t = 1, \dots, T$, and $i, j = 1, \dots, N$
4. Dynamic heterogeneity: the VAR coefficients and the residual variance-covariance matrix are allowed to be period-specific. In other words, $A_{ij,t}^k \neq A_{ij,s}^k$ and $\Sigma_{ij,t} \neq \Sigma_{ij,s}$ when $t \neq s$ for each $k = 1, \dots, p$, and, $i, j = 1, \dots, N$.

As noted by Koop and Korobilis, 2019, the unrestricted panel VAR described is likely to be over-parametrized, involving $p \times (N \times n)^2$ unknown autoregressive parameters and $\frac{N \times n \times (N \times n + 1)}{2}$ error covariance terms. Therefore the following approach developed in Ciccarelli and Canova, 2006, and Canova and Ciccarelli, 2013 is used to produce a restricted version of the general panel VAR. This structural factor approach allows not only for cross-subsectional heterogeneity but also for dynamic and static interdependencies, which are the main properties of interest when working in a panel VAR setup rather than with single VAR models.

Structural factor model

Following Canova and Ciccarelli, 2013 and starting from Equation (3), if we allow for cross-subsectional heterogeneity, static and dynamic interdependency, but ignore dynamic heterogeneity, we obtain the dynamic equation for the full model at period t as:

$$y_t = A^1 y_{t-1} + \cdots + A^p y_{t-p} + C x_t + \varepsilon_t \quad (8)$$

Taking the transpose of the vector of observations and reformulating in compact form, we have:

$$y'_t = \begin{pmatrix} y'_{t-1} & \dots & y'_{t-p} & x'_t \end{pmatrix} \begin{pmatrix} (A^1)' \\ \vdots \\ (A^p)' \\ C' \end{pmatrix} + \varepsilon'_t, \quad (9)$$

or, in stacked form, we define:

$$y'_t = X_t B + \varepsilon'_t, \quad (10)$$

where:

$$X_t = \underbrace{(y'_{t-1} \dots y'_{t-p} \quad x'_t)}_{1 \times k}, \quad B = \begin{pmatrix} (A^1)' \\ \vdots \\ (A^p)' \\ C' \end{pmatrix}. \quad (11)$$

By using the vectorization of the matrix of coefficients B , we refer to:

$$y_t = (I_{Nn} \otimes X_t) vec(B) + \varepsilon_t \quad (12)$$

or:

$$y_t = \bar{X}_t \beta + \varepsilon_t, \quad (13)$$

where:

$$\bar{X}_t = \underbrace{(I_{Nn} \otimes X_t)}_{Nn \times h}, \quad (14)$$

is the matrix containing the lagged observations , and

$$\beta = \underbrace{vec(B)}_{h \times 1} \quad (15)$$

is the vectorized matrix of coefficients that we are intended in estimating.

Since one allows for static interdependencies in the model, the variance-covariance matrix of the residual term ε_t does not have to be block diagonal anymore. In addition, a higher degree of flexibility is permitted by assuming that the error term ε_t follows the distribution described as:

$$\varepsilon_t \sim \mathcal{N}(0, \Sigma),$$

where:

$$\Sigma = \sigma \tilde{\Sigma} = \underbrace{\begin{pmatrix} \sigma \underbrace{\tilde{\Sigma}_{11}}_{n \times n} & \sigma \tilde{\Sigma}_{12} & \dots & \sigma \tilde{\Sigma}_{1N} \\ \sigma \tilde{\Sigma}_{21} & \sigma \tilde{\Sigma}_{22} & \dots & \sigma \tilde{\Sigma}_{2N} \\ \vdots & \vdots & \ddots & \vdots \\ \sigma \tilde{\Sigma}_{N1} & \sigma \tilde{\Sigma}_{N2} & \dots & \sigma \tilde{\Sigma}_{NN} \end{pmatrix}}_{N \times N \times N} = \begin{pmatrix} \underbrace{\Sigma_{11}}_{n \times n} & \Sigma_{12} & \dots & \Sigma_{1N} \\ \Sigma_{21} & \Sigma_{22} & \dots & \Sigma_{2N} \\ \vdots & \vdots & \ddots & \vdots \\ \Sigma_{N1} & \Sigma_{N2} & \dots & \Sigma_{NN} \end{pmatrix} \quad (16)$$

Where σ is a scaling random variable, which can follow an inverse Gamma distribution:

$$\sigma \sim IG\left(\frac{\alpha_0}{2}, \frac{\delta_0}{2}\right), \quad (17)$$

where α_0 and δ_0 are hyperparameters to be defined by the researcher.

Looking closer to Equation (13), one sees that it takes the form of a standard linear model and could in principle be estimated by any standard OLS or Bayesian methods. However, as mentioned before, it suffers from the curse of dimensionality: the number of coefficients is likely to be larger than the size of the data set. The structural factor model assumes that the h elements of the vector of coefficients β can be expressed as a linear function of a much lower number r of structural factors:

$$\beta = \Xi_1 \theta_1 + \Xi_2 \theta_2 + \dots + \Xi_r \theta_r = \sum_{i=1}^r \Xi_i \theta_i, \quad (18)$$

where $\theta_1, \theta_2, \dots, \theta_r$ are vectors of dimension $d_1 \times 1, d_2 \times 1, \dots, d_r \times 1$ containing the structural factors, while $\Xi_1, \Xi_2, \dots, \Xi_r$ are selection matrices of dimensions $h \times d_1, h \times d_2, \dots, h \times d_r$.

$h \times d_2, \dots, h \times d_r$ with all their entries being either 0 or 1 picking the relevant elements in $\theta_1, \theta_2, \dots, \theta_r$. We can define the selection matrices and the structural factors as:

$$\Xi = \underbrace{(\Xi_1 \quad \Xi_2 \quad \dots \quad \Xi_r)}_{h \times d}, \quad \theta = \underbrace{\begin{pmatrix} \theta_1 \\ \theta_2 \\ \vdots \\ \theta_r \end{pmatrix}}_{d \times 1}. \quad (19)$$

Thus, we can rewrite Equation (18) in compact form as:

$$\beta = \Xi\theta. \quad (20)$$

If we substitute in Equation (13), then we obtain a reformulated model as:

$$\begin{aligned} y_t &= \bar{X}_t \beta + \varepsilon_t \\ &= \bar{X}_t \Xi \theta + \varepsilon_t \\ &= (\bar{X}_t \Xi) \theta + \varepsilon_t \\ &= \tilde{X}_t \theta + \varepsilon_t, \end{aligned} \quad (21)$$

where:

$$\tilde{X}_t = \underbrace{\bar{X}_t \Xi}_{N \times d} \quad (22)$$

Is a reparametrization of the lagged observation that depends on the selection matrix. However, when dealing with a panel VAR model, identification strategy for the models is applied as follows:

- A factor θ_1 is used to capture a common component. It thus always comprises $d_1 = 1$ coefficient.

- A factor θ_2 is used to capture components which are specific to the unit to which belongs the explained variable. As there are $N = 9$ countries in the panel, θ_2 is composed of $d_2 = 9$ coefficients.
- A factor θ_3 is used to capture components which are specific to the explained variable itself. Model 1 has *electricity price* as the only endogenous variable, therefore $n = 1$, so θ_3 comprises $d_3 = 1$ coefficient. Model 2 (BVAR + RES) and Model 3 (BVARX) include unit-specific series for forecasted RES generation for solar, wind, and load; despite not being endogenous variables themselves, to keep the model parsimonious a single common coefficient is estimated for each and excluding one factor, in this case *load*, to avoid collinearity issues with θ_1 . In this sense, $d_3 = 3$ for the last two models.
- A factor θ_4 is used to capture lag-specific components. Each equation includes p lags, but in order to avoid collinearity issues with the common component θ_1 , θ_4 comprise $d_4 = p - 1$ coefficients. For all models, lags are restricted to $t - 1$, $t - 2$, and $t - 7$, which correspond to one day, two days, and one week before the delivery time, as suggested in the literature (Knittel and Roberts, 2005, Raviv et al., 2015, and Weron and Misiorek, 2008) who show how these specifications capture the seasonal patterns in electricity prices. This lag structure is represented by $p = 3$, hence $d_4 = 2$.
- A factor θ_5 is used to capture exogenous variable components. As m represents the number of exogenous variables on each model, θ_5 comprises $d_5 = m$ coefficients. In this application, the intercept and dummy variables are treated as exogenous variables. Model 1 (BVAR) and Model 2 (BVAR + RES) include $m = 13$ exogenous variables: intercept, dummies for each month (except December, to avoid collinearity issues), weekends and holidays (only for BVAR+RES and BVARX); Model 3 (BVARX) includes $m = 19$ exogenous variables, as international prices for oil, gas, coal and CO2 are added on top of the dummies.

The definition of the series Ξ_1 , Ξ_2 , Ξ_3 , Ξ_4 , and Ξ_5 are illustrated for Model 1 only,

as for the other two models the structure is similar. Considering the structure of the first model, there are $N = 9$ units, $n = 1$ endogenous variables, $p = 3$ lags and $m = 13$ exogenous variables (intercept + dummies), thus the model is represented as:

$$\begin{aligned}
 \underbrace{\begin{pmatrix} y_{11,t} \\ y_{21,t} \\ \vdots \\ y_{91,t} \end{pmatrix}}_{9 \times 1} &= \underbrace{\begin{pmatrix} a_{11,t}^1 & a_{12,t}^1 & \dots & a_{19,t}^1 \\ a_{21,t}^1 & a_{22,t}^1 & \dots & a_{29,t}^1 \\ \vdots & \vdots & \ddots & \vdots \\ a_{91,t}^1 & a_{11,t}^1 & \dots & a_{99,t}^1 \end{pmatrix}}_{9 \times 9} \underbrace{\begin{pmatrix} y_{11,t-1} \\ y_{21,t-1} \\ \vdots \\ y_{91,t-1} \end{pmatrix}}_{9 \times 1} + \dots \\
 &+ \underbrace{\begin{pmatrix} a_{11,t}^7 & a_{12,t}^7 & \dots & a_{19,t}^7 \\ a_{21,t}^7 & a_{22,t}^7 & \dots & a_{29,t}^7 \\ \vdots & \vdots & \ddots & \vdots \\ a_{91,t}^7 & a_{11,t}^7 & \dots & a_{99,t}^7 \end{pmatrix}}_{9 \times 9} \underbrace{\begin{pmatrix} y_{11,t-7} \\ y_{21,t-7} \\ \vdots \\ y_{91,t-7} \end{pmatrix}}_{9 \times 1} + \dots \\
 &+ \underbrace{\begin{pmatrix} c_{11,t} & c_{12,t} & \dots & c_{113,t} \\ c_{21,t} & c_{22,t} & \dots & c_{213,t} \\ \vdots & \vdots & \ddots & \vdots \\ c_{91,t} & c_{11,t} & \dots & c_{913,t} \end{pmatrix}}_{9 \times 13} \underbrace{\begin{pmatrix} x_{1,t} \\ x_{2,t} \\ \vdots \\ x_{13,t} \end{pmatrix}}_{13 \times 1} + \underbrace{\begin{pmatrix} \varepsilon_{1,t} \\ \varepsilon_{2,t} \\ \vdots \\ \varepsilon_{13,t} \end{pmatrix}}_{9 \times 1}
 \end{aligned} \tag{23}$$

The single common factor component implies that $\theta_1 = (\theta_{11})$. There are nine units, so $\theta_2 = (\theta_{21}, \theta_{22}, \dots, \theta_{29})'$. There is one endogenous variable so that $\theta_3 = (\theta_{31})$. There are 3 lags, so $\theta_4 = (\theta_{41}, \theta_{42})'$. Finally, 13 exogenous variables gives $\theta_5 = (\theta_{51} \ \theta_{52}, \dots, \theta_{513})'$, which sums up to $d = 42$ coefficients to estimate. Also, the model comprises $h = Nn(Nnp + m) = 378$ coefficients to be estimated at time t. The dimensions of the selection matrices are: Ξ_1 is $h \times d_1$ or 378×1 , Ξ_2 is $h \times d_2$ or 378×9 , Ξ_3 is $h \times d_3$ or 378×1 , Ξ_4 is $h \times d_4$ or 378×2 , Ξ_5 is $h \times d_5$ or 378×13 .

Consider the explained variable $y_{11,t}$. As it belongs to unit 1, it would be represented as:

$$\begin{aligned}
y_{11,t} = & \left(\sum_{k=1}^p \sum_{i=1}^N y_{i1,t-k} + \sum_{i=1}^m x_{i,t} \right) \theta_{11} + \left(\sum_{k=1}^p y_{11,t-k} \right) \theta_{21} + \left(\sum_{k=1}^p \sum_{i=1}^N y_{i1,t-k} \right) \theta_{31} + \\
& \left(\sum_{i=1}^N y_{i1,t-1} \right) \theta_{41} + \left(\sum_{i=1}^N y_{i1,t-2} \right) \theta_{42} + \sum_{i=1}^m x_{i1,t} \theta_{5i} + \varepsilon_{1,t},
\end{aligned} \tag{24}$$

or in stacked form as:

$$y_{11,t} = \mathcal{Z}_{11}\theta_{11} + \mathcal{Z}_{21}\theta_{21} + \mathcal{Z}_{31}\theta_{31} + \mathcal{Z}_{41}\theta_{41} + \mathcal{Z}_{42}\theta_{42} + \sum_{i=1}^m \mathcal{Z}_{5i}\theta_{5i} + \varepsilon_{1,t} \tag{25}$$

where:

- $\mathcal{Z}_{11} = \sum_{p=1}^p \sum_{i=1}^N y_{i1,t-p} + \sum_{i=1}^m x_{i,t}$ represents the common component of the model. It includes all the explanatory variables $k = 42$.
- $\mathcal{Z}_{21} = \sum_{p=1}^p y_{11,t-p}$ represents the component specific to unit 1, therefore it includes all the values corresponding to that unit, which are, in this case, 3 (one for each lag).
- $\mathcal{Z}_{31} = \sum_{p=1}^p \sum_{i=1}^N y_{i1,t-p}$ represents the component specific to the endogenous variable, therefore includes the $N \times p$ values for electricity prices .
- $\mathcal{Z}_{41} = \sum_{i=1}^N y_{i1,t-1}$ represents the component specific to the first lag variable, therefore it includes the N values of $p = 1$.
- $\mathcal{Z}_{42} = \sum_{i=1}^N y_{i1,t-2}$ represents the component specific to the second lag variable, therefore it includes the N values of $p = 2$.
- $\mathcal{Z}_{5i} = \sum_{i=1}^m x_{i1,t}$ represents the contribution of all the dummies $m = 13$, which are measured separately, as they depend on t and not on the unit.

Continuing with the other $N - 1$ equations, the model can be rewritten in compact form as:

$$\begin{aligned}
& \underbrace{\begin{pmatrix} y_{11,t} \\ y_{21,t} \\ \vdots \\ y_{91,t} \end{pmatrix}}_{N \times 1} = \\
& \underbrace{\begin{pmatrix} \mathcal{Z}_{11,t} & \mathcal{Z}_{21,t} & 0 & \dots & 0 & \mathcal{Z}_{31,t} & \mathcal{Z}_{41,t} & \mathcal{Z}_{42,t} & \mathcal{Z}_{51,t} & \dots & \mathcal{Z}_{513,t} \\ \mathcal{Z}_{11,t} & 0 & \mathcal{Z}_{22,t} & \dots & 0 & \mathcal{Z}_{31,t} & \mathcal{Z}_{41,t} & \mathcal{Z}_{42,t} & \mathcal{Z}_{51,t} & \dots & \mathcal{Z}_{513,t} \\ \vdots & \vdots & \vdots & \ddots & \vdots & \vdots & \vdots & \vdots & \vdots & \ddots & \vdots \\ \mathcal{Z}_{11,t} & 0 & 0 & \dots & \mathcal{Z}_{29,t} & \mathcal{Z}_{31,t} & \mathcal{Z}_{41,t} & \mathcal{Z}_{42,t} & \mathcal{Z}_{51,t} & \dots & \mathcal{Z}_{513,t} \end{pmatrix}}_{N \times d} + \\
& \underbrace{\begin{pmatrix} \theta_{11} \\ \theta_{21} \\ \theta_{22} \\ \vdots \\ \theta_{29} \\ \theta_{31} \\ \theta_{41} \\ \theta_{42} \\ \theta_{51} \\ \vdots \\ \theta_{513} \end{pmatrix}}_{d \times 1} \\
& \underbrace{\begin{pmatrix} \varepsilon_{11,t} \\ \varepsilon_{21,t} \\ \vdots \\ \varepsilon_{91,t} \end{pmatrix}}_{N \times 1}
\end{aligned} \tag{26}$$

or:

$$y_t = \mathcal{Z}_t \theta + \varepsilon_t, \quad (27)$$

with:

$$\mathcal{Z}_t = \underbrace{\begin{pmatrix} \mathcal{Z}_{11,t} & \mathcal{Z}_{21,t} & 0 & \dots & 0 & \mathcal{Z}_{31,t} & \mathcal{Z}_{41,t} & \mathcal{Z}_{42,t} & \mathcal{Z}_{51,t} & \dots & \mathcal{Z}_{513,t} \\ \mathcal{Z}_{11,t} & 0 & \mathcal{Z}_{22,t} & \dots & 0 & \mathcal{Z}_{31,t} & \mathcal{Z}_{41,t} & \mathcal{Z}_{42,t} & \mathcal{Z}_{51,t} & \dots & \mathcal{Z}_{513,t} \\ \vdots & \vdots & \vdots & \ddots & \vdots & \vdots & \vdots & \vdots & \vdots & \ddots & \vdots \\ \mathcal{Z}_{11,t} & 0 & 0 & \dots & \mathcal{Z}_{29,t} & \mathcal{Z}_{31,t} & \mathcal{Z}_{41,t} & \mathcal{Z}_{42,t} & \mathcal{Z}_{51,t} & \dots & \mathcal{Z}_{513,t} \end{pmatrix}}_{N \times d} \quad (28)$$

Comparing Equation (21) with Equation (28), one obtains:

$$\bar{X}_t \Xi = \mathcal{Z}_t \quad (29)$$

The series of matrices Ξ must be defined so that Equation (29) holds. For Model 1, the series of matrices $\Xi_1, \Xi_2, \Xi_3, \Xi_4$, and Ξ_5 must be defined as:

$$\begin{aligned} \Xi_1 &= \underbrace{\begin{pmatrix} \mathbf{1}_{42} \\ \mathbf{1}_{42} \\ \vdots \\ \mathbf{1}_{42} \end{pmatrix}}_{h \times 1} & \Xi_2 &= \underbrace{\begin{pmatrix} \nu_1 & \mathbf{0}_{42} & \dots & \mathbf{0}_{42} \\ \mathbf{0}_{42} & \nu_2 & \dots & \mathbf{0}_{42} \\ \vdots & \ddots & \ddots & \vdots \\ \mathbf{0}_{42} & \mathbf{0}_{42} & \dots & \nu_9 \end{pmatrix}}_{h \times N} & \Xi_3 &= \underbrace{\begin{pmatrix} \nu_{10} \\ \nu_{10} \\ \vdots \\ \nu_{10} \end{pmatrix}}_{h \times 1} \\ \Xi_4 &= \underbrace{\begin{pmatrix} \nu_{11} & \nu_{12} \\ \nu_{11} & \nu_{12} \\ \vdots & \vdots \\ \nu_{11} & \nu_{12} \end{pmatrix}}_{h \times (p-1)} & \Xi_5 &= \underbrace{\begin{pmatrix} \nu_{13} & \nu_{14} & \dots & \nu_{28} \\ \nu_{13} & \nu_{14} & \dots & \nu_{28} \\ \vdots & \ddots & \ddots & \vdots \\ \nu_{13} & \nu_{14} & \dots & \nu_{28} \end{pmatrix}}_{h \times m} \end{aligned} \quad (30)$$

Where $\mathbf{1}_n$ and $\mathbf{0}_n$ respectively denote a $n \times 1$ vector of ones and zeros, and $\nu_1, \nu_2, \dots, \nu_{28}$ are the selection vectors $\nu_{i,i} \in \{0, 1\}$ of the $k = 42$ variables available.

Hence:

$$\Xi = \underbrace{\begin{pmatrix} \mathbf{1}_{42} & \nu_1 & \mathbf{0}_{42} & \dots & \mathbf{0}_{42} & \nu_{10} & \nu_{11} & \nu_{12} & \nu_{13} & \nu_{14} & \dots & \nu_{28} \\ \mathbf{1}_{42} & \mathbf{0}_{42} & \nu_2 & \dots & \mathbf{0}_{42} & \nu_{10} & \nu_{11} & \nu_{12} & \nu_{13} & \nu_{14} & \dots & \nu_{28} \\ \vdots & \vdots & \ddots & \vdots & \ddots & \vdots \\ \mathbf{1}_{42} & \mathbf{0}_{42} & \mathbf{0}_{42} & \dots & \nu_9 & \nu_{10} & \nu_{11} & \nu_{12} & \nu_{13} & \nu_{14} & \dots & \nu_{28} \end{pmatrix}}_{h \times d} \quad (31)$$

This concludes the specification of the static factor approach for Model 1. Applying the same procedure Model 2 and 3 were designed. Because \tilde{X}_t can be computed for each period t once Ξ is defined, it is possible to stack Equation (21) over the T periods and estimate the model directly from OLS or a Bayesian approach.

Model estimation

Following Dieppe et al., 2016, Ciccarelli and Canova, 2006, and Canova and Ciccarelli, 2013, from a Bayesian perspective, the goal is to recover the posterior distribution for the three parameters of interest: θ , $\tilde{\Sigma}$, and σ . Then it will be possible to draw values for θ and thus for β from Equation (20). And combining a draw for $\tilde{\Sigma}$ with a draw from σ , one may recover a draw for Σ .

Assuming independence between θ , $\tilde{\Sigma}$, and σ and applying the Bayes rule, the posterior distribution for the parameters would be:

$$\pi(\sigma, \tilde{\Sigma}, \sigma | y) \propto f(y | \sigma, \tilde{\Sigma}, \sigma) \pi(\theta) \pi(\tilde{\Sigma}) \pi(\sigma) \quad (32)$$

In particular, Equation (32) states that the posterior distribution is obtained by combining the likelihood of the data $f(y | \sigma, \tilde{\Sigma}, \sigma)$ with the respective prior distributions for θ , $\tilde{\Sigma}$, and σ , respectively given by $\pi(\theta)$, $\pi(\tilde{\Sigma})$, and, $\pi(\sigma)$. Taking Equation (16) and replacing it in the likelihood function, one obtains:

$$f(y | \sigma, \tilde{\Sigma}, \sigma) \propto (\sigma)^{-TNn/2} |\tilde{\Sigma}|^{-T/2} \prod_{t=1}^T \left\{ \exp \left(-\frac{1}{2} \sigma^{-1} (y_t - \tilde{X}_t \theta)' \tilde{\Sigma}^{-1} (y_t - \tilde{X}_t \theta) \right) \right\}, \quad (33)$$

The prior distributions for θ , $\tilde{\Sigma}$, and σ are considered as follows. Prior for θ is a multivariate normal distribution with mean θ_0 and variance Θ_0 , which in formula is equal to:

$$\pi(\theta | \theta_0, \Theta_0) \propto \exp \left(-\frac{1}{2} (\theta - \theta_0)' \Theta_0^{-1} (\theta - \theta_0) \right). \quad (34)$$

For $\tilde{\Sigma}$, we assume a Wishart prior as denoted in the following equation:

$$\pi(\tilde{\Sigma}) \propto |\tilde{\Sigma}|^{-Nn+1/2}. \quad (35)$$

Finally, as already stated, σ follows an inverse Gamma distribution with shape $\frac{\alpha_0}{2}$ and scale $\frac{\delta_0}{2}$, which in formula is:

$$\pi(\sigma) \propto \sigma^{-\frac{\alpha_0}{2}-1} \exp\left(\frac{-\delta_0}{2\sigma}\right). \quad (36)$$

Using the Bayes rule for the posterior distribution defined in Equation (32), and combining the likelihood in Equation (33) with the priors denoted in Equations (34),(35), and (36), the joint posterior distribution is:

$$f(\theta, \tilde{\Sigma}, \sigma | y) \propto \prod_{t=1}^T \left\{ \exp\left(-\frac{1}{2}\sigma^{-1}(y_t - \tilde{X}\theta)' \tilde{\Sigma}^{-1}(y_t - \tilde{X}\theta)\right) \right\} \times \exp\left(\frac{-\delta_0}{2\sigma}\right) \\ \times (\sigma)^{-NnT+\alpha_0/2-1} \times \exp|\tilde{\Sigma}|^{-(T+Nn+1)/2} \times \exp\left(-\frac{1}{2}(\theta - \theta_0)' \Theta_0^{-1}(\theta - \theta_0)\right) \quad (37)$$

since the joint posterior distribution in Equation (37) is not in closed form, we rely on the conditional posterior distributions. In particular, the conditional posterior distribution of θ is obtained after relegating any term not involving θ from Equation (37) to the proportionality constant. One obtains:

$$\pi(\theta | y, \sigma, \tilde{\Sigma}) \propto \exp\left(-\frac{1}{2}(\theta - \bar{\theta})' \bar{\Theta}^{-1}(\theta - \bar{\theta})\right) \quad (38)$$

with:

$$\bar{\Theta} = \left(\tilde{X} I_\Sigma \tilde{X}' + \Theta_0^{-1} \right) \quad (39)$$

and

$$\bar{\theta} = \bar{\Theta} \left(\tilde{X} I_\Sigma y + \Theta_0^{-1} \theta_0 \right) \quad (40)$$

with:

$$\tilde{X} = \underbrace{\begin{pmatrix} \tilde{X}'_1 & \tilde{X}'_2 & \dots & \tilde{X}'_T \end{pmatrix}}_{d \times NnT},$$

$$I_\Sigma = (I_T \otimes \Sigma^{-1}) = \underbrace{\begin{pmatrix} \Sigma^{-1} & 0 & \dots & 0 \\ 0 & \Sigma^{-1} & & 0 \\ \vdots & & \ddots & \vdots \\ 0 & 0 & \dots & \Sigma^{-1} \end{pmatrix}}_{NnT \times NnT}, \quad y = \underbrace{\begin{pmatrix} y_1 \\ y_2 \\ \vdots \\ y_T \end{pmatrix}}_{NnT \times 1}, \quad (41)$$

This is the kernel of a multivariate normal distribution with mean $\bar{\theta}$ and covariance matrix $\bar{\Theta}$:

$$\pi(\theta|y, \sigma, \tilde{\Sigma}) \sim \mathcal{N}(\bar{\theta}, \bar{\Theta}). \quad (42)$$

Following the same procedure, the conditional posterior for $\tilde{\Sigma}$ is equal to:

$$\pi(\tilde{\Sigma}|y, \theta, \sigma) \propto |\tilde{\Sigma}|^{-(T+Nn+1)/2} \exp\left(-\frac{1}{2} \text{tr}\{\tilde{\Sigma}^{-1} \bar{S}\}\right), \quad (43)$$

with:

$$\bar{S} = \sigma^{-1} \left(Y - \ddot{X} I_0 \right) \left(Y - \ddot{X} I_0 \right)' \quad (44)$$

where:

$$Y = \underbrace{\begin{pmatrix} y_1 & y_2 & \dots & y_T \end{pmatrix}}_{Nn \times T}, \quad \ddot{X} = \underbrace{\begin{pmatrix} \tilde{X}_1 & \tilde{X}_2 & \dots & \tilde{X}_T \end{pmatrix}}_{Nn \times dT}$$

$$I_0 = (I_T \otimes \theta) = \underbrace{\begin{pmatrix} \theta & 0 & \dots & 0 \\ 0 & \theta & & 0 \\ \vdots & & \ddots & \vdots \\ 0 & 0 & \dots & \theta \end{pmatrix}}_{Td \times T}, \quad (45)$$

This is the kernel of an inverse Wishart distribution with scale \bar{S} and T degrees of freedom:

$$\pi(\tilde{\Sigma}|y, \theta, \sigma) \sim \mathcal{IW}(\bar{S}, T) \quad (46)$$

Finally, we obtain the conditional posterior for σ . Relegating to the proportionality constant any term not involving σ in Equation (37), then rearranging, it is obtained:

$$\pi(\sigma|y, \theta, \tilde{\Sigma}) \propto (\sigma)^{-\frac{\bar{\alpha}}{2}-1} \exp\left(-\frac{\bar{\delta}}{2\sigma}\right) \quad (47)$$

with:

$$\bar{\alpha} = NnT + \alpha_0 \quad (48)$$

and:

$$\bar{\delta} = \left[\text{tr} \left((Y - \ddot{X} I_\theta)(Y - \ddot{X} I_\theta)' \tilde{\Sigma}^{-1} \right) + \delta_0 \right] \quad (49)$$

This is the kernel of an inverse Gamma distribution with shape $\frac{\bar{\alpha}}{2}$ and scale $\frac{\bar{\delta}}{2}$:

$$\pi(\sigma|y, \theta, \tilde{\Sigma}) \sim \mathcal{IG}\left(\frac{\bar{\alpha}}{2}, \frac{\bar{\delta}}{2}\right) \quad (50)$$

Now that the conditional posterior distributions have been characterized, the Gibbs sampling algorithm can be described as follows:

1. Define starting values $\theta^{(0)}$, $\tilde{\Sigma}^{(0)}$ and $\sigma^{(0)}$. $\theta^{(0)}$ and $\tilde{\Sigma}^{(0)}$ come from their OLS estimation, while for $\sigma^{(0)}$, the value is set to 1, which implies $\Sigma^{(0)} = \tilde{\Sigma}^{(0)}$. Then compute $I_{\Sigma}^{(0)} = I_T \otimes (\Sigma^{(0)})^{-1}$ and $I_{\theta}^{(0)} = I_T \otimes \theta^{(0)}$
2. At iteration n , draw $\tilde{\Sigma}^{(n)}$ from $\pi(\tilde{\Sigma}^{(n)} | y, \theta^{n-1}, \sigma^{n-1}) \sim \mathcal{IW}(\bar{S}, T)$, with:

$$\bar{S} = (\sigma^{(n-1)})^{-1} (Y - \ddot{X} I_{\theta}^{(n-1)}) (Y - \ddot{X} I_{\theta}^{(n-1)})'$$
3. At iteration n , draw $\sigma^{(n)}$ from $\pi(\sigma^{(n)} | y, \theta^{(n-1)}, \tilde{\Sigma}^{(n-1)}) \sim \mathcal{IG}\left(\frac{\bar{\alpha}}{2}, \frac{\bar{\delta}}{2}\right)$ with:

$$\bar{\alpha} = NnT + \alpha_0$$

and:

$$\bar{\delta} = \left[\text{tr}((Y - \ddot{X} I_{\theta}^{(n-1)})(Y - \ddot{X} I_{\theta}^{(n-1)})'(\tilde{\Sigma}^{(n)})) + \delta_0 \right]$$
4. At iteration n , compute $\Sigma^{(n)} = \sigma^{(n)} \tilde{\Sigma}^{(n)}$, and use it to compute $I_{\Sigma}^{(n)} = I_T \otimes (\Sigma^{(n)})^{-1}$.
5. At iteration n , draw $\theta^{(n)}$ from $\pi(\theta^{(n)} | y, \sigma^{(n)}, \tilde{\Sigma}^{(n)}) \sim \mathcal{N}(\bar{\theta}, \bar{\Theta})$, with:

$$\bar{\Theta} = (\tilde{X} I_{\sigma}^{(n)} \tilde{X}' + \Theta_0^{-1})$$

and:

$$\bar{\theta} = \bar{\Theta} \left(\tilde{X} I_{\sigma}^{(n)} y + \Theta_0^{-1} \theta_0 \right)^{-1}$$
6. At iteration n , compute $I_{\theta}^{(n)} = I_T \otimes \theta^{(n)}$.
7. Repeat until the algorithm reach convergence.

4 Empirical Results

In Sample

First, results for the in-sample period estimation are shown. The in-sample period ranges from January 1st, 2020 to December 31st 2021. The panel VARs were estimated using the Gibbs Sampler algorithm described in the previous section, with 10,000 iterations and a burn-in of 2,000. Results of the mean posterior distributions for the coefficients are shown in Table 3.

Table 3: In-sample posterior mean coefficients

Coefficient	BVAR	BVAR + RES	BVARX
Common factor	2.31	0.01	0.02
Belgium	0.05	0.01	0.01
Denmark	-0.18	0.005	0.01
Finland	-0.001	0.01	0.01
France	0.1	0.01	0.01
Germany	-0.06	0.01	0.01
Italy	0.12	0.01	0.01
Netherlands	0.11	0.01	0.01
Portugal	0.01	0.01	0.01
Spain	0.08	0.01	0.01
Elec. price	-2.28	0.03	0.01
Solar $t - 1$	-	0.01	0.01
Wind $t - 1$	-	0.01	0.01
Elec. price $t - 1$	-0.01	0.07	0.06
Elec. price $t - 7$	-0.02	0.01	0.02
Oil $t - 1$	-	-	-0.12
Gas $t - 1$	-	-	0.57
Coal $t - 1$	-	-	0.24
CO2 $t - 1$	-	-	-0.06

Intercept	15.01	-65.85	-95.99
Jan	-0.69	-4.40	-2.95
Feb	-2.93	0.07	3.66
Mar	-6.97	1.92	5.74
Apr	-6.17	7.92	15.24
May	-5.61	8.71	16.59
Jun	-7.81	5.16	18.20
Jul	0.37	1.53	14.14
Aug	3.24	6.56	15.35
Sep	9.36	5.20	15.02
Oct	5.06	7.06	7.17
Nov	4.78	5.33	6.08
Weekends	-7.56	5.85	11.46
Holidays	-	4.68	16.90

Coefficients for the Bayesian Panel VAR attribute certain effect to the unit-specific component of the model, being Italy (0.12) the country with the highest coefficient and Denmark (-0.18) with the lowest coefficient. The endogenous variable, including all its lags has an estimated coefficient of -2.28, meaning that, on average, for each price unit that the lagged prices increases, current price would decrease by 2.28 EUR/hour, indicating the high persistence of these autoregressive processes. Lagged prices registered coefficients with considerably lower values.

Regarding the dummies, from February to July all coefficients estimated were negative, while the other half of the year registered positive effects on the electricity prices. March and June are the months with the highest negative impact on price, while, on the other hand, September and October are the ones with the highest positive impact. The coefficient for weekends indicates to lower prices by 7.56 EUR/hour, on average. It is worth mentioning that several chains of the posterior distribution of the coefficients are skewed and seem to be bi-modal.

When forecasted day-ahead RES generation series are included, unit-specific effects for all units are estimated to be considerable lower if compared against the first model. Endogenous variable coefficient changes to 0.03 from -2.28 when RES were not included. Intercept value and sign changed considerably, from 15.01 in the last model to -65.85 in this one. Dummies turned to have all positive effect, except for January; with the highest value estimated for April and May, and the lowest values for July and February. This sort of behavior in the coefficients seem to indicate that day-ahead RES generation forecast explain part of the unit-specific effects and the seasonal dummies relevance, being RES generation highly seasonal itself.

It is puzzling the fact that despite its inclusion, RES coefficients are as low as the unit-specific coefficients. Another result worth noticing is how the posterior chains turned into a normal distribution shaped curved when estimating the BVAR + RES model.

Finally, the BVARX model, which includes fuel and CO2 prices as exogenous variables shows a similar behavior in the coefficients for countries, day-ahead RES generation and electricity price and its lags, as in Model 2. Regarding the exogenous variables, lagged Gas and Coal prices affect positively the electricity price by 0.57 and 0.24 EUR/hour upon one EUR increase on their price. Conversely, Oil and CO2 show a negative effect of -0.12 and -0.06 EUR/hour by the same measurement.

Dummies coefficients got all higher values. BVARX model dummies' coefficients seem to show a stronger seasonality towards the middle of the year than the other models, all with positive signs, indicate a higher electricity price for the units from April to September and a lower price in the rest of the year. Coefficients for weekends and Holidays were estimated at higher values than the other models.

Out of sample - Forecasting

The out of sample analysis consists in performing a rolling window day-ahead forecast for the out-of-sample period that ranges from January 1st 2021 to September 30th 2023. This implies a slight modification of the Gibbs Sampler algorithm described in Section 3. The key difference is that the algorithm is now run up to $T_{forecast} = 637$ times, to produce the day-ahead forecast for each day of the out-of-sample period. To reduce the computational burden, the number of iterations is set to 2,000 with a burn-in of 500. Figures 9, 10, and 11 show the forecast of the three different models for each country.

To assess the forecasts performance, following Gianfreda et al., 2023 two criteria are adopted, first one is a point metric, the root-mean-squared-error for each of the days forecasted (RMSE), which is computed as follows for unit i :

$$RMSE_i = \sqrt{\frac{1}{T} \sum_{t=R}^{T-1} (\hat{y}_{i,t+1} - y_{i,t+1})^2} \quad (51)$$

where T is the number of observations of the out-of-sample period, R is the length of the rolling window and \hat{y}_{t+1} are the daily forecasted electricity prices. The overall RMSE of each model is computed by averaging for the units altogether, to have a single comparison metric per model.

The second metric to asses the goodness of the forecasts is a density measure, the continuous ranked probability score (CRPS) (Gneiting and Raftery, 2007). This density measure, as noted in Gianfreda et al., 2023, rewards better the values from the predictive density that are close to - but not equal to - the outcome, and they are less sensitive to outliers. The CRPS is interpreted as the lower the number, the better the score, and it is given by:

$$CRPS_{i,t}(y_{i,t+1}) = \int_{-\infty}^{\infty} (F(z) - I\{y_{i,t+1} \leq z\})^2 dz = \\ E_f |Y_{i,t+1} - y_{i,t+1}| - 0.5E_f |Y_{i,t+1} - Y'_{i,t+1}| \quad (52)$$

where F denotes the cumulative distribution function associated with the predictive density f , $I\{y_{i,t+1} \leq z\}$ denotes an indicator function taking the value 1 if $y_{i,t+1} \leq z$ and 0 otherwise, and $Y_{i,t+1}$ and $Y'_{i,t+1}$ are independent random draws from the posterior predictive density.

Then, a one-sided Diebold and Mariano test (Diebold and Mariano, 1995) is performed to determine if models 2 (BVAR + RES) and 3 (BVARX) differences in forecast accuracy against model 1 (BVAR) are significant, using RMSE and CRPS scores as losses for each country. The p-values of each test is computed using Newey-West standard errors to account for the autocorrelation present in the forecast by the rolling window set up. As noted by Clark and West, 2007 and Clark and McCracken, 2012, the Diebold and Mariano test is conservative and might result in under-rejection of the null hypothesis of equal predictability.

Finally, the Model Confidence Set (MCS) procedure proposed by Hansen et al., 2011 is employed to determine the set of models with higher predictive power for each country, both for RMSE and CRPS scores. The MCS is a test of set of models that is constructed such that it will contain the 'best' forecasting model, given a level of confidence.

Results

Results of both the RMSE and CRPS measures on the forecasting performance of the three panels are shown in Table 4. The models forecasting performance is tested on each unit individually and the full panel. Considering the RMSE point measure, values range widely for the three panels tested, with a standard deviation of 12.8 for the BVAR, 14.4 for the BVAR+RES and 16.8 for the BVARX. The BVAR and BVAR+RES models registered the same average RMSE (64.4), but the BVARX performed only slightly worse (65.4) although it was expected better forecasting capabilities from it.

For the BVAR panel, the best performance is registered on Denmark (49.2) and Italy (52.7), while the best performance for the BVAR+RES and BVARX was on the

Netherlands (44.5 and 43.1) and Belgium (47.6 and 47.1). For the BVAR panel, highest RMSE was registered on Finland (85.6) and Germany (80.6), while for the BVAR+RES and BVARX panels, it was both Portugal (80.4 and 86.9) and Spain (80.7 and 87.4).

Against the benchmark model (BVAR), BVAR+RES had the largest reduction in RMSE in Germany by 28.6 points, followed by the Netherlands with 20.8 points and Belgium with 17.3 points. Similarly, the BVARX model registered the best improvement in Germany, the Netherlands and Belgium, with a reduction of 28.1, 22.1, and 17.8 points, respectively. On the other hand, largest increase in RMSE for both BVAR+RES and BVARX models was registered in Spain, Portugal and Italy: Spain increased its RMSE by 27.1 and 33.8 points, Portugal by 26.9 and 33.4 points, and Italy by 14.4 and 8.7 points.

Table 4: Forecasting metrics for panel VAR models

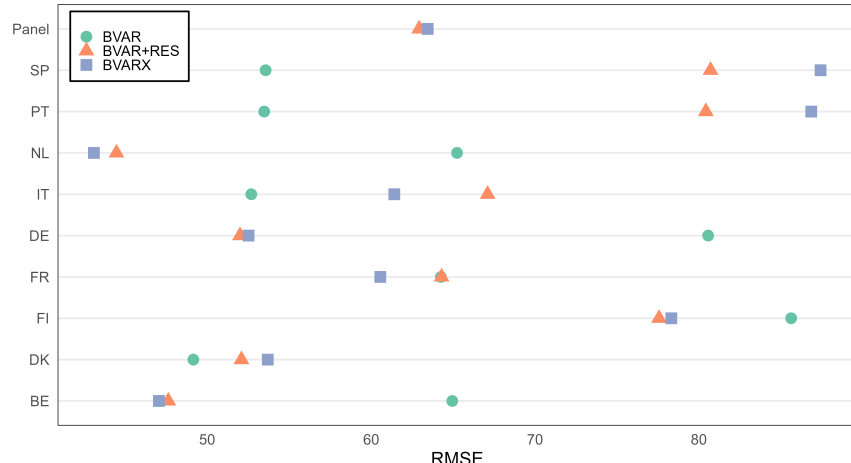
Unit	BVAR		BVAR + RES		BVARX	
	RMSE	CRPS	RMSE	CRPS	RMSE	CRPS
Belgium	64.9	34.1	47.6	27.0	47.1	26.6
Denmark	49.2	28.8	52.1	29.2	53.7	30.3
Finland	85.6	46.7	77.6	44.1	78.3	44.0
France	64.2	33.7	64.3	36.0	60.6	33.3
Germany	80.6	40.8	52.0	29.5	52.5	30.1
Italy	52.7	28.0	67.1	38.4	61.4	34.6
Netherlands	65.2	34.1	44.5	25.0	43.1	24.6
Portugal	53.5	29.1	80.4	43.6	86.9	47.9
Spain	53.6	29.3	80.7	43.8	87.4	48.5
Panel avg	64.4	33.8	64.4	35.2	65.4	35.5

Regarding the CRPS score, results show a similar pattern as the RMSE analysis. Here, the benchmark model registered a value of 33.8, with the BVAR+RES model scoring a value 1.4 points higher, and the BVARX a value 1.7 points higher as well.

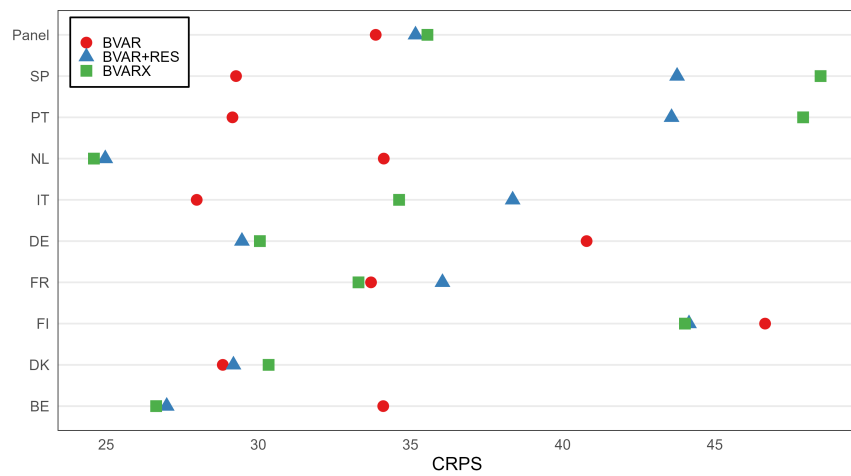
For the benchmark model, best performance was achieved in Italy (28.0) and Denmark (28.8), while the highest CRPS was registered in Finland (46.7) and Germany (40.8). On its side, BVAR+RES performed better on the Netherlands (25.0) and worst on Spain (43.8) and Portugal (43.6); similar results were shown by the BVARX, with Netherlands (24.6) with the lowest score and the countries from the Iberian peninsula with the highest: Spain, 48.5, and Portugal, 47.9.

Against the benchmark model, BVAR+RES registered a CRPS improvement of 11.3 points for Germany, 9.1 for the Netherlands, and 7.1 for Belgium, while the largest increase in absolute CRPS was in Spain, Portugal, and Italy, with 14.5, 14.5 and 10.4 points, respectively. BVARX had largest increase in performance for Germany (10.7), the Netherlands (9.5) and Belgium (7.5) and the largest decrease in performance for Spain (19.2), Portugal (18.8), and Italy (6.6).

For Finland, Denmark and France, both for RMSE and CRPS measures, results were very similar throughout the three models. Indicating how little information is provided by RES, fuels, and CO₂ when included in their forecasts. On the other hand, it is clearly visible how countries from southern Europe (Italy, Portugal, and Spain) are not as sensible to these additional variables as the countries from central Europe (Belgium, Germany, the Netherlands). It would be interesting to study deeper the reason why France is not on this latter group.



(a) RMSE



(b) CRPS

Figure 8: Forecast performance measures, point metric RMSE (top) and density metric CRPS (bottom)

To assess if the BVAR+RES and BVARX models are statistically better than the benchmark, the Diebold and Mariano test was performed. Table 5 shows the p-values of the Diebold and Mariano test of the benchmark BVAR model against the BVAR+RES and BVARX models. The Diebold and Mariano test p-values suggest that there is not enough evidence to reject the null hypothesis -the two forecasting models have the same forecasting accuracy- for any country, both using the RMSE and the CRPS evaluation metrics.

Table 5: Diebold and Mariano test p-values, with BVAR model as benchmark

Unit	BVAR RES		BVAR X	
	RMSE	CRPS	RMSE	CRPS
Belgium	0.384	0.409	0.396	0.422
Denmark	0.492	0.504	0.506	0.516
Finland	0.469	0.483	0.471	0.484
France	0.496	0.525	0.465	0.496
Germany	0.394	0.405	0.411	0.420
Italy	0.572	0.589	0.525	0.556
Netherlands	0.372	0.395	0.382	0.403
Portugal	0.586	0.597	0.609	0.610
Spain	0.587	0.596	0.612	0.612

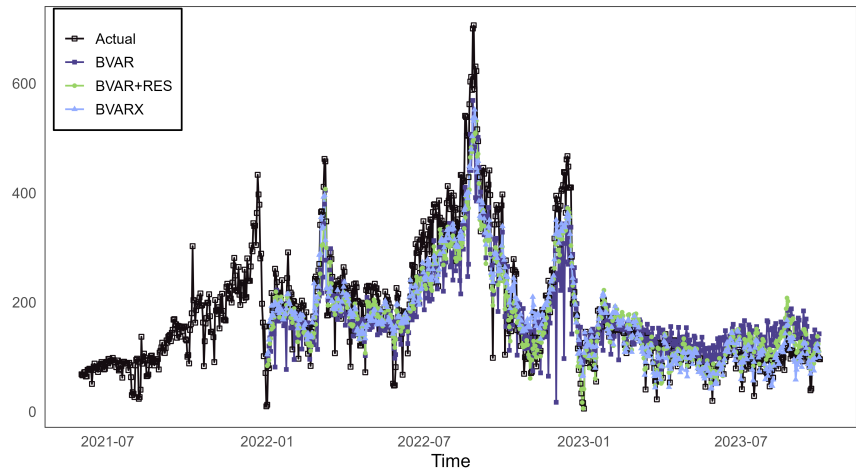
Finally, the Model Confidence Set procedure was applied both for RMSE and CRPS metrics, results are in Table 6 and are the same in practical terms. Concerning both RMSE and CRPS metrics, results differ according to the country tested. For Denmark, Finland, and France, all models have equal predictive power, for Belgium, Germany, and the Netherlands, models 2 (BVAR+RES) and 3 (BVARX) have better predictive power than model 1 (BVAR); For Italy, model 2 was excluded and for Portugal and Spain, only model 1 is in their confidence sets.

Table 6: Model Confidence Set (MCS) and corresponding p-values for each unit.

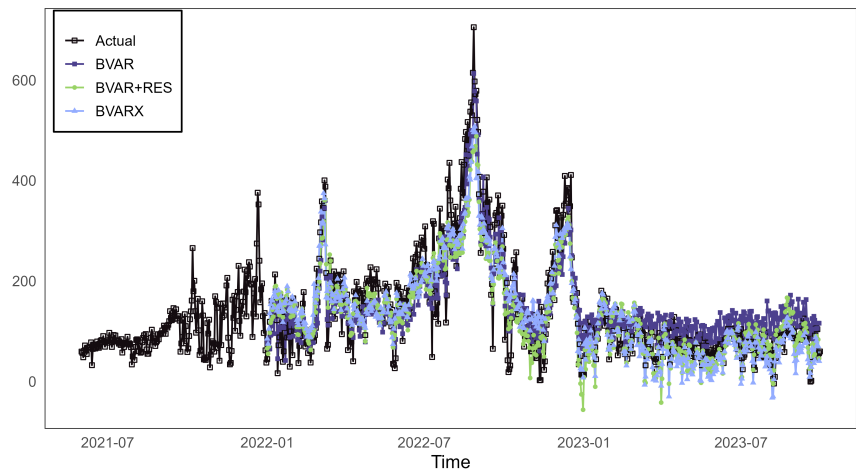
Unit	RMSE		CRPS	
	MCS	p-value	MCS	p-value
Belgium	M2, M3	0.506	M2, M3	0.766
Denmark	M1, M2, M3	0.469	M1, M2, M3	0.247
Finland	M1, M2, M3	0.275	M1, M2, M3	0.591
France	M1, M2, M3	0.540	M1, M2, M3	0.153
Germany	M2, M3	0.204	M2, M3	0.425
Italy	M1, M3	0.422	M1, M3	0.095*
Netherlands	M2, M3	0.509	M2, M3	0.583
Portugal	M1	0.005***	M1	0.009***
Spain	M1	0.012**	M1	0.009***

Confidence levels: * < 10%, ** < 5%, *** < 1%.

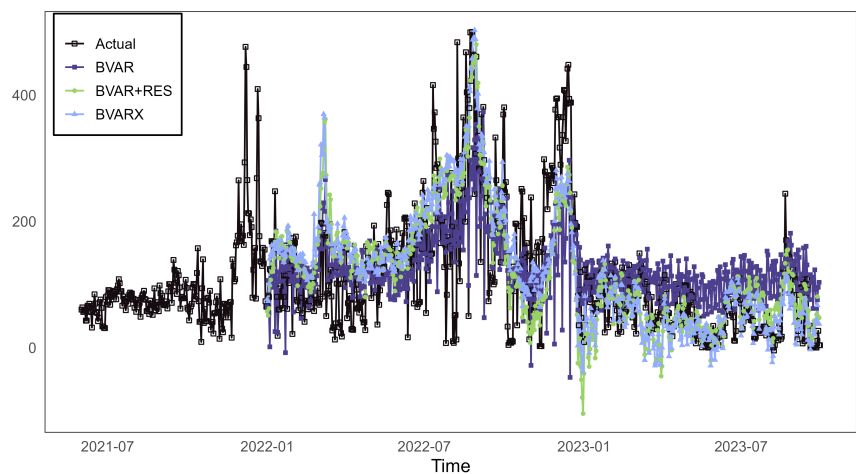
Figures 9, 10, 11 show the out-sample period of electricity prices and the forecasted electricity prices from each model, for each country.



(a) Belgium

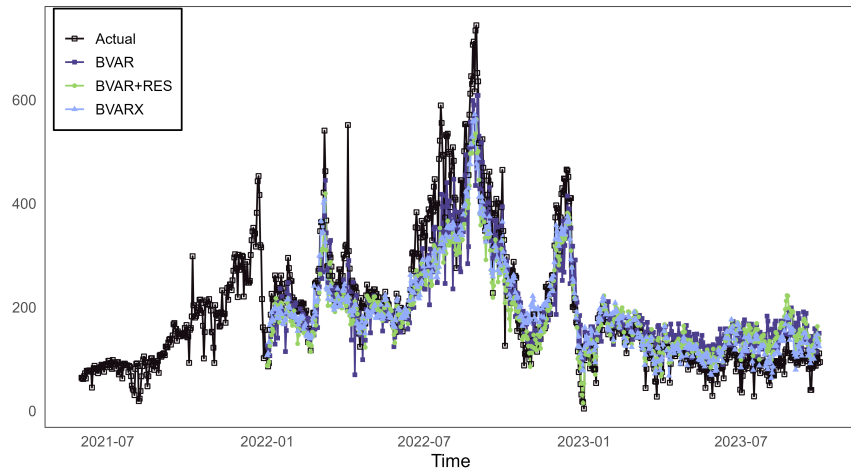


(b) Denmark

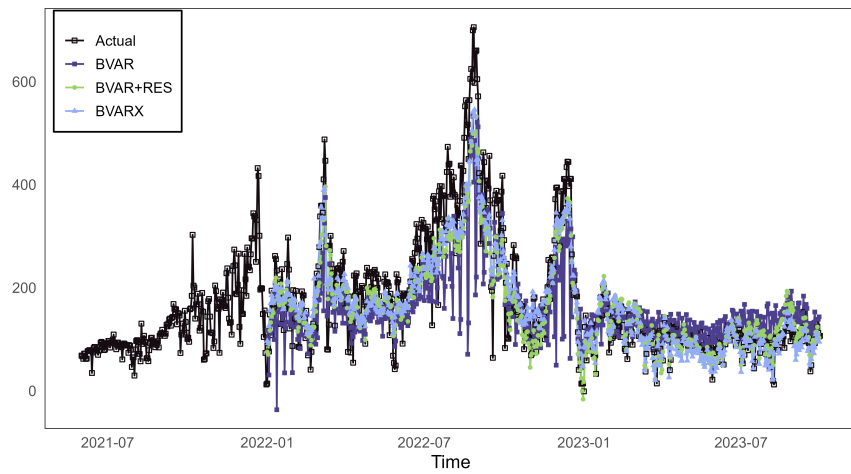


(c) Finland

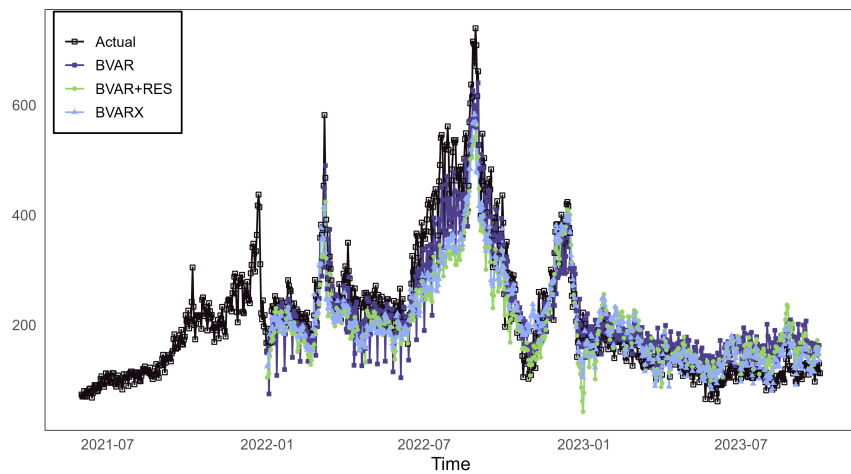
Figure 9: Electricity price forecasts per country: BE, DK, FI



(a) France

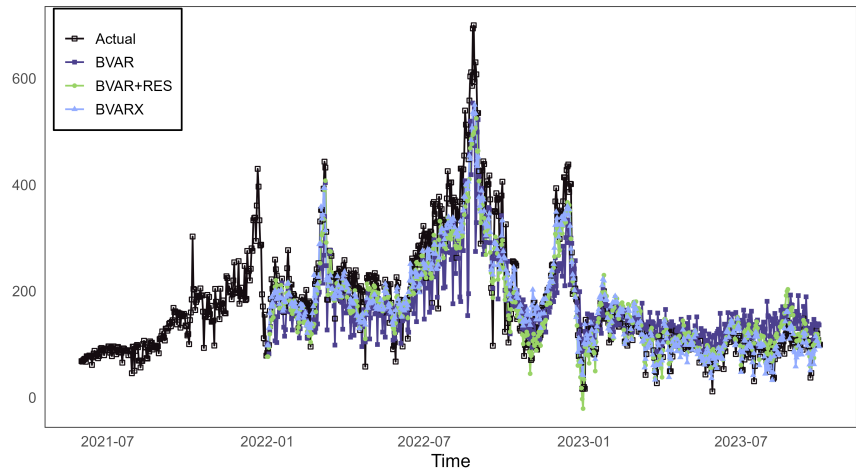


(b) Germany

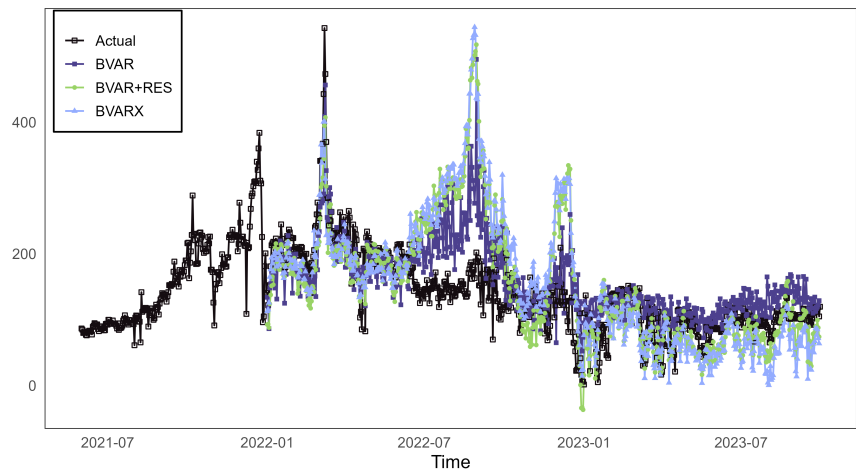


(c) Italy

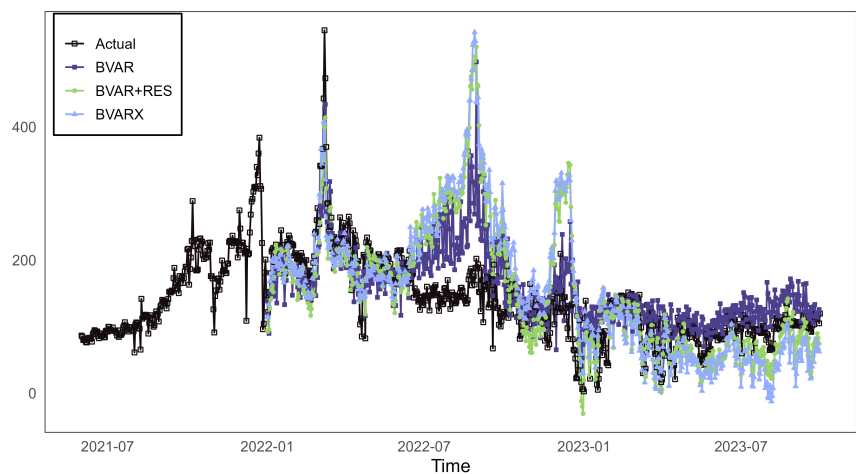
Figure 10: Electricity price forecasts per country: FR, DE, IT



(a) Netherlands



(b) Portugal



(c) Spain

Figure 11: Electricity price forecasts per country: NL, PT, SP

5 Conclusions

The goal of this study was to complement the ongoing discussion about electricity markets in Europe, how they are interconnected and what kind of models could be applied to improve their forecasting. For this purpose, a panel dataset of electricity prices, forecasted RES generation and international fuels and CO₂ prices was created. The panel is composed of nine countries and ranges from January 1st 2020 to September 30th 2023, with daily-frequency data. From this dataset, daily electricity price was modeled through three different panel VAR models using a Bayesian approach. To address the curse of dimensionality that the panel VARs present, a structural factor approach with static interdependencies presented in Dieppe et al., 2016 was implemented.

The three models were then analyzed in two different fashions. First, the vector of posterior mean coefficients was estimated for the in-sample period and then discussed as well as the posterior mean variance-covariance matrix of residuals. Second, rolling window day-ahead forecasts were produced for the out-sample period and tested through the Diebold and Mariano test and Model Confidence Set both for point and density measures.

The main findings with respect to the in-sample analysis are the unit-specific effects in the panel for the BVAR model, although these coefficients resulted in lesser values for the other two models. It was expected a clearer view of the cross-subsectional heterogeneity in the coefficients for the BVAR+RES and BVARX models. Nevertheless, the dynamic interdependencies were evident and showed the autoregressive nature of the electricity prices in all models; dummies' coefficients changed considerably throughout the estimations, both in direction as well as in magnitude.

Regarding the forecasts, performance varies greatly between countries. For Portugal and Spain, it is clear how these two markets are different from the rest of the panel, also, the benchmark model proved to be statistically the best model for them. For the rest of the countries, no statistical significance was achieved to determine

improvements from the benchmark model. Nevertheless, both point and density metrics indicated the similar performance of the models for Belgium, Germany and the Netherlands, while France and Italy showed some mixed results. All of this is evidence of how strong the geographical span of a country and its proximity to other markets is when analysing its prices.

To continue this line of study, the focus could be centered on more sophisticated models such as time-varying (TV) coefficient panel VARs or MIDAS models. Extending this study to estimate hourly electricity prices could be of interest or to include the rest of the Nordic countries (Norway and Sweden) and estimate these models for regional panels (Central Europe, Iberian peninsula, Nordics) and compare the results against a full panel like the one tested here. Finally, testing different combinations of explanatory variables is always interesting, as there is usually hourly or daily data on electricity generation per technology, transfer capacities, allocations and day, week, and month ahead forecasts. There is plenty of paths to explore, especially during these times when topics such as the energy and electricity markets are becoming more and more attractive to the population in general, and more critical to economists and policy makers.

Acknowledgements

I would like to express my gratitude to my advisor, Luca Rossini, who introduced me to the world of Bayesian Statistics and guided me through all the stages of my thesis. Thanks to him, I challenged myself to develop a work that I could have only imagined at the beginning of this year. Professor Rossini's passion and love for his field encouraged me to give my best in every delivery.

I am also grateful to the University, for granting me the opportunity to be part of this program and making this academic journey possible; for my professors across various courses, who encouraged me to explore and learn from state-of-the art applications in economics, statistics, machine learning, and many others fields; to my colleagues, for warmly welcoming me into their lives, sharing with me part of their tradition and culture, and engaging in enriching academic discussions.

Finally, to my biggest supporter, my mother Sandra, who has backed me in every endeavor I would pursue and that has lifted me up whenever I needed it. To my family and friends in Colombia and Europe, who were by my side since I decided to pursue a new academic degree, who believed in me and gave me their best when I needed it. To all of them, I owe a big debt of gratitude.

Bibliography

References

- Diebold, F. X., & Mariano, R. S. (1995). Comparing predictive accuracy. *Journal of Business and Economic Statistics*, 13(3), 253–263.
- Knittel, C. R., & Roberts, M. R. (2005). An empirical examination of restructured electricity prices. *Energy Economics*, 27(5), 791–817.
- Ciccarelli, M., & Canova, F. (2006). *Estimating Multi-country VAR models* (tech. rep.). Society for Computational Economics.
- Clark, T. E., & West, K. D. (2007). Approximately normal tests for equal predictive accuracy in nested models. *Journal of Econometrics*, 138(1), 291–311.
- Gneiting, T., & Raftery, A. E. (2007). Strictly proper scoring rules, prediction, and estimation. *Journal of the American Statistical Association*, 102(477), 359–378.
- Weron, R., & Misiorek, A. (2008). Forecasting spot electricity prices: A comparison of parametric and semiparametric time series models. *International Journal of forecasting*, 24(4), 744–763.
- Hansen, P. R., Lunde, A., & Nason, J. M. (2011). The model confidence set. *Econometrica*, 79(2), 453–497.
- Clark, T. E., & McCracken, M. W. (2012). Reality checks and comparisons of nested predictive models. *Journal of Business & Economic Statistics*, 30(1), 53–66.
- Canova, F., & Ciccarelli, M. (2013). Panel Vector Autoregressive Models: A Survey. In *Var models in macroeconomics—new developments and applications: Essays in honor of christopher a. sims* (pp. 205–246). Emerald Group Publishing Limited.
- Raviv, E., Bouwman, K. E., & Van Dijk, D. (2015). Forecasting day-ahead electricity prices: Utilizing hourly prices. *Energy Economics*, 50, 227–239.
- Dieppe, A., Legrand, R., & Van Roye, B. (2016). The BEAR toolbox.
- Koop, G., & Korobilis, D. (2019). Forecasting with high-dimensional panel VARs. *Oxford Bulletin of Economics and Statistics*, 81(5), 937–959.

- Durante, F., Gianfreda, A., Ravazzolo, F., & Rossini, L. (2022). A multivariate dependence analysis for electricity prices, demand and renewable energy sources. *Information Sciences*, 590, 74–89.
- Foroni, C., Ravazzolo, F., & Rossini, L. (2023). Are low frequency macroeconomic variables important for high frequency electricity prices? *Economic Modelling*, 120, 106160.
- Gianfreda, A., Ravazzolo, F., & Rossini, L. (2023). Large Time-Varying Volatility Models for Hourly Electricity Prices. *Oxford Bulletin of Economics and Statistics*, 85(3), 545–573.
- Uniejewski, B. (2023). Smoothing Quantile Regression Averaging: A new approach to probabilistic forecasting of electricity prices. *arXiv preprint arXiv:2302.00411*.

Appendix

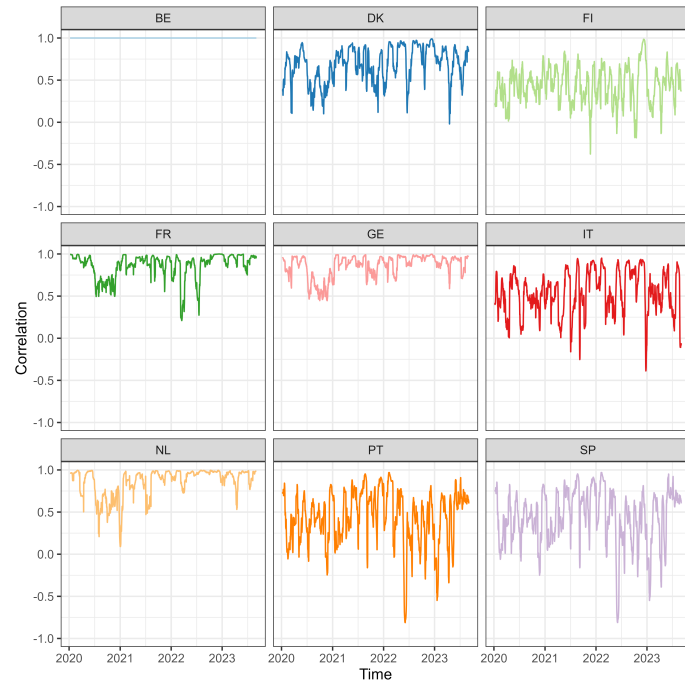


Figure 12: Rolling-window correlation coefficients, full-sample period [2020-2023]: Belgium

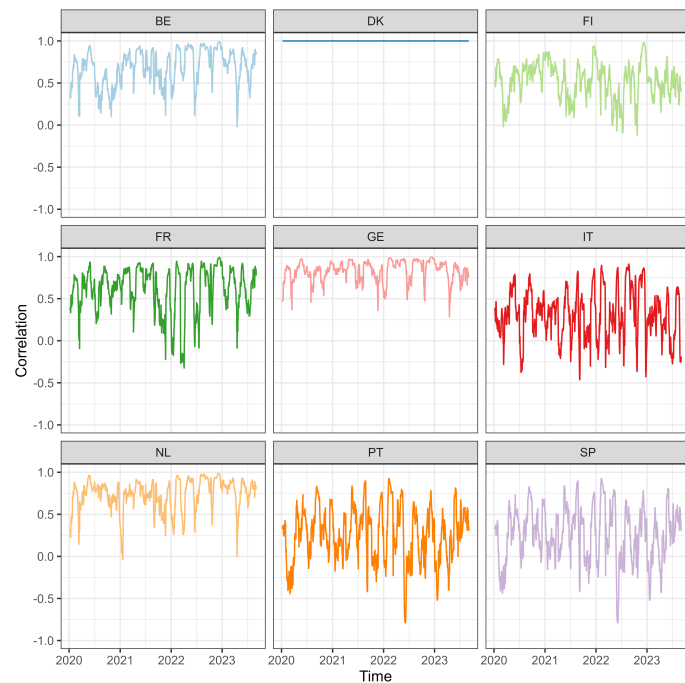


Figure 13: Rolling-window correlation coefficients, full-sample period [2020-2023]: Denmark

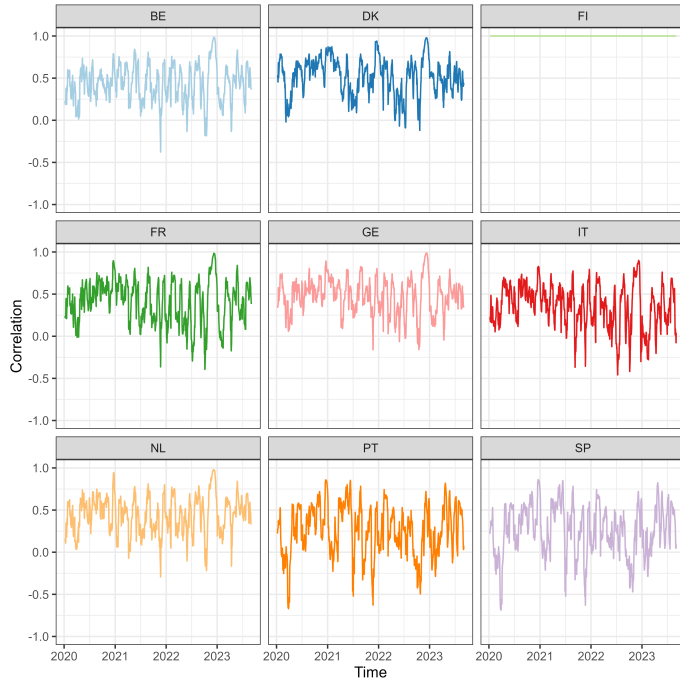


Figure 14: Rolling-window correlation coefficients, full-sample period [2020-2023]: Finland

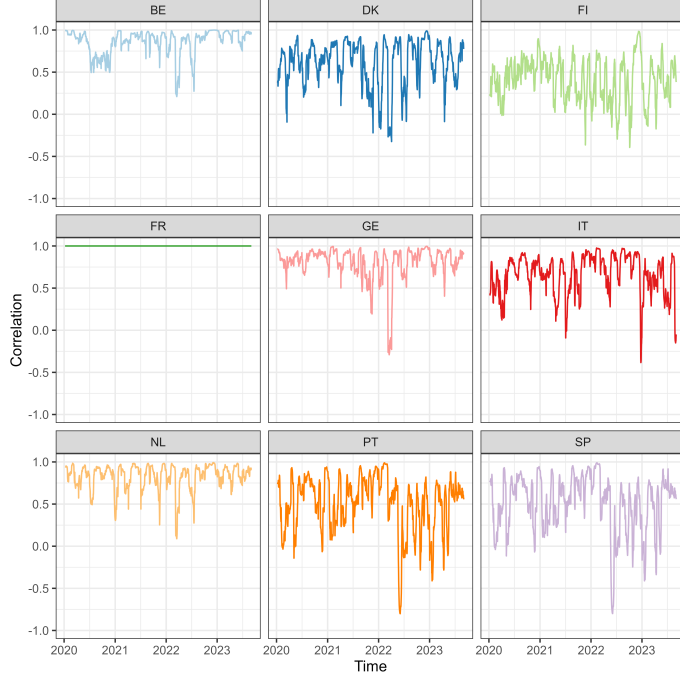


Figure 15: Rolling-window correlation coefficients, full-sample period [2020-2023]: France

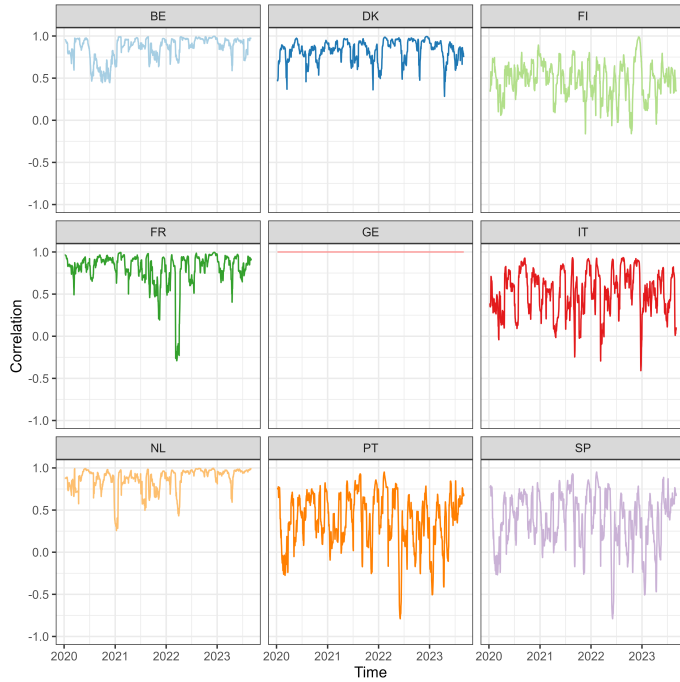


Figure 16: Rolling-window correlation coefficients, full-sample period [2020-2023]: Germany

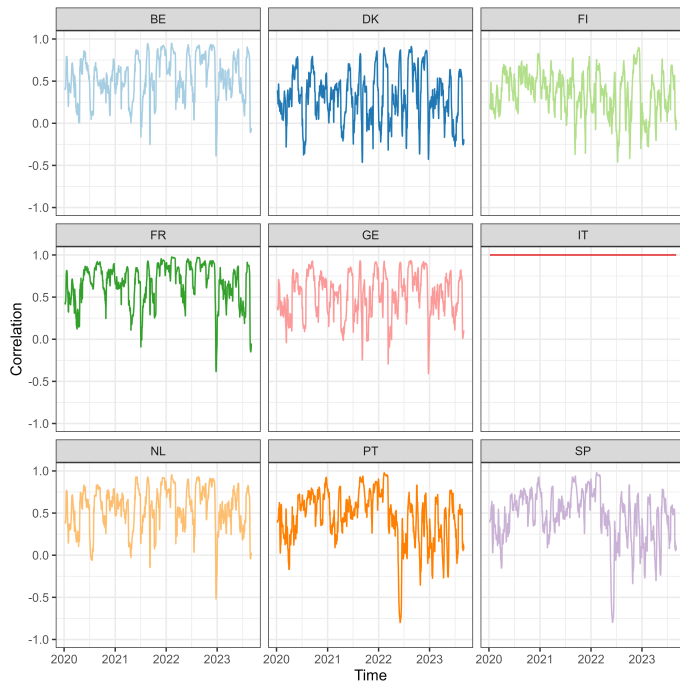


Figure 17: Rolling-window correlation coefficients, full-sample period [2020-2023]: Italy

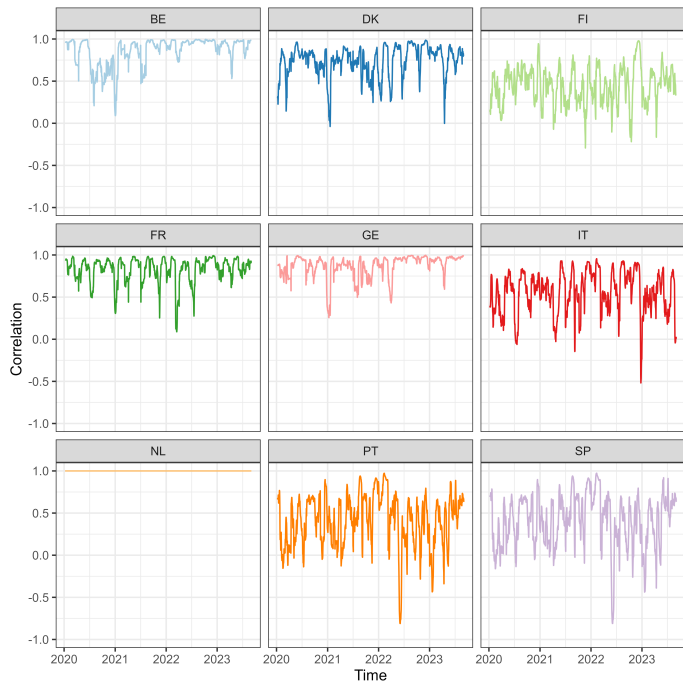


Figure 18: Rolling-window correlation coefficients, full-sample period [2020-2023]: Netherlands

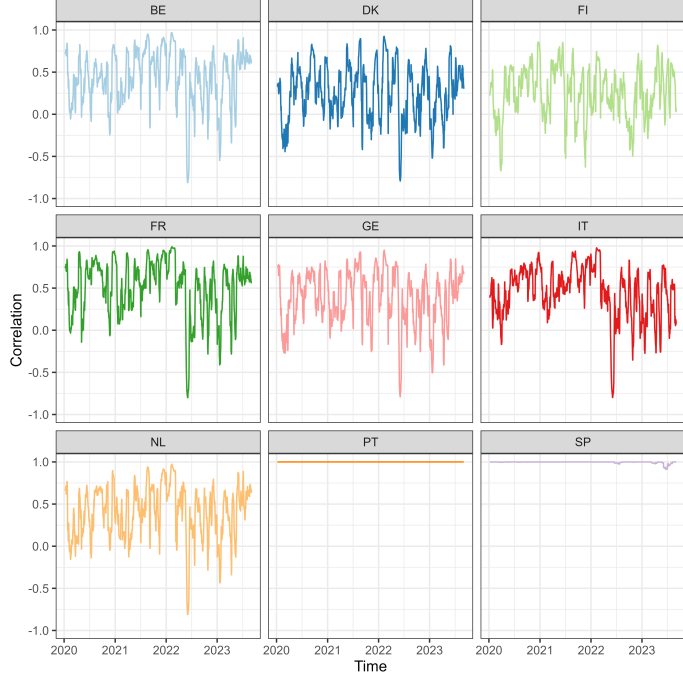


Figure 19: Rolling-window correlation coefficients, full-sample period [2020-2023]: Portugal

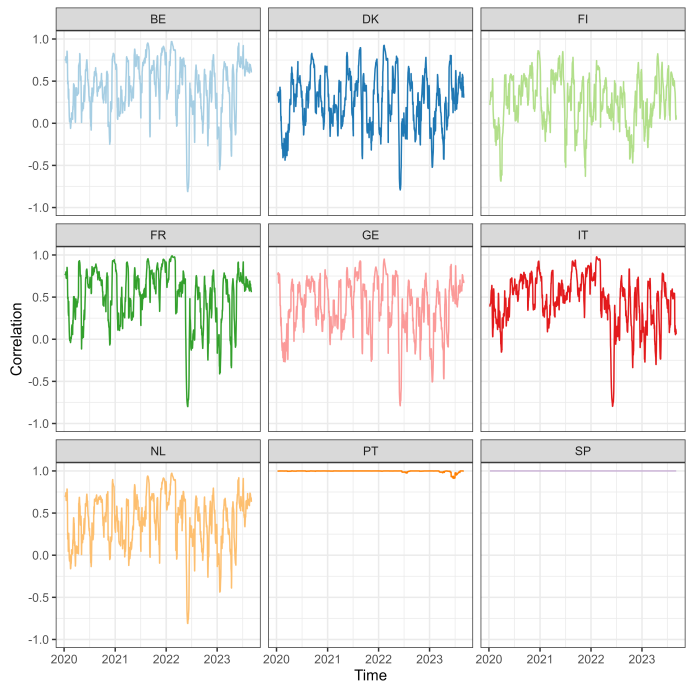


Figure 20: Rolling-window correlation coefficients, full-sample period [2020-2023]: Spain